Faculdade de Engenharia da Universidade do Porto

Unravelling the Mechanism of Action of Antimicrobial Peptides when Conjugated to Nanoparticles

Francisco Alves Pereira Rodrigues

September, 2022

Faculdade de Engenharia da Universidade do Porto

Instituto de Ciências Biomédicas Abel Salazar

Unravelling the Mechanism of Action of Antimicrobial Peptides when Conjugated to Nanoparticles

Francisco Alves Pereira Rodrigues

Dissertation accomplished in the context of the

Masters in Biomedical Engineering

Supervisor: Cláudia Monteiro, PhD
I3S – Instituto de Investigação e Inovação em Saúde, Universidade do Porto, Porto, Portugal

Co-Supervisor: Cláudia Pinho, PhD
LAQV, REQUIMTE – Faculdade de Farmácia, Universidade do Porto, Porto, Portugal

Co-Supervisor: Cristina Martins, PhD
I3S – Instituto de Investigação e Inovação em Saúde, Universidade do Porto, Porto, Portugal

September, 2022

Abstract

Antibiotic-resistant bacteria are considered by the World Health Organization one of the biggest threats to healthcare and food security nowadays and are rapidly spreading all around the world, causing already around 700,000 deaths globally per year, according to a 2019 report from the United Nations. In this context, alternatives to antibiotics are in urgent need.

One alternative treatment that seems to have the potential to fight these infections are antimicrobial peptides (AMPs). These peptides are ubiquitous in all forms of life, present a broad-spectrum of antimicrobial activity, and appear to have a low probability of inducing resistance, due to their mechanism of action. Nonetheless, AMPs still present several drawbacks when applied *in vivo*. Conjugation with nanoparticles is one technique that has been explored in the past years to overcome some of those challenges and has already been demonstrated in multiple studies that it can improve AMPs stability and protect them against degradation.

One example of this type of conjugation was performed by our group when the AMP MSI-78(4-20), a derivative from pexiganan, was grafted to poly(lactide-co-glycolide acid)-polyethylene glycol (PLGA-PEG) nanoparticles (NPs) through covalent binding. Using this strategy, the bactericidal activity of the AMP was improved by accelerating the killing kinetics of the AMP at bactericidal concentrations. However, no information is available about how conjugation to NPs can affect the mechanism of action of AMPs and more specifically no studies have been developed with the system developed by our group. To assess this, interaction studies in simplified models mimicking the bacterial membranes need to be conducted.

In this context, we used models mimicking the membranes of Gram-positive and Gram-negative bacteria, more specifically giant unilamellar vesicles (GUVs), to study the mechanisms of action of MSI-78(4-20) when grafted to NPs of PLGA-PEG. This was done by confocal laser scanning microscopy using fluorescently labelled AMP-NPs and fluorescently labelled membrane mimetic models.

The addition of fluorescence to the particles did not interfere with their size, surface charge, or with the grafting of the AMP, as confirmed by dynamic and electrophoretic light scattering and AMP quantification. The GUVs were produced by electroformation of a 1,2-dioleoyl-*sn*-glycero-3-phosphatidylcholine (DOPC) and 1-palmitoyl-2-oleoyl-*sn*-glycero-3-phosphatidylglycerol (POPG) mixture to mimic Gram-Positive bacteria, while a mixture of

DOPC, POPG, and lipopolysaccharide (LPS) was used for GUVs resembling Gram-negative bacterial membranes. GUVs characterization and optimization was evaluated through inverted fluorescence microscopy.

Interactions between free AMP, bare NPs and AMP-NPs with the GUVs were followed by Confocal microscopy and images were recorded in time-lapse. The bare NPs showed no interaction with the GUVs, maintaining their original shape for both GUVs mimicking Gram-Positive and Gram-Negative bacteria, also some aggregation was observed for higher concentrations. Both AMP and AMP-NPs exhibited signs of interaction with both type of GUVs. The AMP induced deformation and aggregation of the GUVs before disrupting their membrane for both types of GUVs, while the AMP-NPs seem to have these effects only for the GUVs mimicking Gram-Negative membranes, disrupting the membrane of GUVs mimicking Gram-Positive bacteria completely without inducing deformation and aggregation. Moreover, AMP-NPs seem to interact at lower concentrations and at a faster rate than the AMP. Another aspect to be noted, was that the interaction for both AMP and AMP-NPs appeared to be slower for the GUVs mimicking Gram-Negative bacteria when comparing to the Gram-Positive model. It was also possible to demonstrate that AMP-NPs accumulated in the membrane of GUVs, by performing a fluorescence intensity profile. This phenomenon is promoted by electrostatic interactions between the negatively charged GUVs and positively charged AMPs.

Resumo

Atualmente, as bactérias resistentes a antibióticos são consideradas pela Organização Mundial de Saúde uma das principais ameaças aos cuidados médicos e à segurança alimentar. Estas bactérias estão a propagar-se rapidamente e a uma escala mundial, provocando aproximadamente 700.000 mortes por ano, de acordo com o relatório de 2019 das Nações Unidas. Assim, é urgente encontrar alternativas a antibióticos.

Um tratamento alternativo que aparenta ter potencial para combater estas infeções são os péptidos antimicrobianos (AMPs). Estes péptidos estão presentes em todas as formas de vida, apresentam um largo espectro de atividade antimicrobiana e aparentam ter pouca probabilidade de adquirir resistência devido ao seu mecanismo de ação. Contudo, os AMPs apresentam diversas desvantagens quando aplicados *in vivo*. Conjugá-los com nanopartículas é uma técnica que tem vindo a ser explorada nos últimos anos, de modo a ultrapassar alguns destes desafios, tendo já demonstrado, em múltiplos estudos, uma melhor estabilidade dos AMPs e proteção dos mesmos de degradação proteolítica.

Um exemplo deste tipo de conjugação foi desenvolvido pelo nosso grupo. O trabalho consistiu na imobilização do AMP MSI-78(4-20), um derivado do pexiganan, em nanopartículas de poly(lactide-co-glycolide acid)-polyethylene glycol (PLGA-PEG), a partir de uma ligação covalente. Aplicando esta estratégia, a atividade bactericida do AMP foi melhorada, ao acelerar a cinética de morte em comparação com o AMP livre. No entanto, não existe informação disponível acerca de como a conjugação com nanopartículas pode afetar o mecanismo de ação dos AMPs e, mais especificamente, não existem estudos para o sistema desenvolvido pelo nosso grupo. Assim, de forma a estudar a interação do AMP imobilizado foram usados neste trabalho modelos simples que mimetizam as membranas das bactérias.

Neste contexto, foram usados modelos que mimetizam as membranas de bactérias Gram-positivas e Gram-negativas, mais especificamente vesículas unilamelares gigantes (GUVs), para estudar os mecanismos de ação do MSI-78(4-20), quando imobilizado em nanopartículas de PLGA-PEG. Este estudo foi realizado observando através de um microscópio confocal de varrimento, a interação do conjugado de AMPs e nanopartículas com modelos que mimetizam membranas de bactérias, ambos marcados com fluorescência.

A adição da molécula fluorescente às partículas não interferiu com o tamanho, carga de superfície, ou com a imobilização dos AMPs, tendo sido estes parâmetros comprovados através de espalhamento de luz dinâmico e eletroforético e pela quantificação do AMP. Os GUVs foram produzidos por eletroformação a partir de uma mistura de 1,2-dioleoyl-*sn*-glycero-3-

phosphatidylcholine (DOPC) e 1-palmitoyl-2-oleoyl-*sn*-glycero-3-phosphatidylglycerol (POPG), para mimetizar bactérias Gram-positivas, enquanto que uma mistura de DOPC, POPG e lipopolissacarídeos (LPS) foi usada para GUVs que mimetizaram as membranas de bactérias Gram-negativas. A caracterização e otimização dos GUVs foi avaliada através de um microscópio invertido de fluorescência.

As interações entre os GUVs e o AMP livre, nanopartículas simples e o conjugado de AMP e nanopartículas, foram estudadas através de microscópica confocal e as imagens obtidas foram gravadas em *time-lapse*. As nanopartículas simples não demonstraram qualquer interação com os GUVs, mantendo estes a sua forma original, quer para os GUVs que mimetizaram bactérias Gram-positivas e Gram-negativas, demonstraram ainda alguma agregação a concentrações mais elevadas. Por outro lado, quer o AMP livre, quer os AMPs conjugados com nanopartículas, apresentaram sinais de interação com os dois tipos de GUVs. O AMP livre induziu deformação e agregação dos GUVs antes de romper a membrana de ambos os tipos, enquanto o conjugado de AMP com nanopartículas apresentou estes efeitos apenas para os GUVs que mimetizaram as bactérias Gram-negativas, rompendo completamente apenas as membranas dos GUVs que mimetizaram as bactérias Gram-positivas, sem induzir deformação e agregação. Adicionalmente, o conjugado demonstrou interagir a mais baixas concentrações e a uma velocidade maior quando comparado com o AMP livre. Foi concluído também que a interação, quer para o AMP livre quer para o conjugado de AMP com nanopartículas, foi mais lenta para os GUVs que mimetizaram as bactérias Gram-negativas, em comparação com os que mimetizaram as bactérias Gram-positivas. Foi possível também demonstrar que o conjugado de AMP com nanopartículas fica acumulado nas membranas dos GUVs, ao realizar um perfil de intensidades de fluorescência. Este fenómeno é promovido por interações eletroestáticas entre os GUVs que são carregados negativamente e os AMPs que possuem carga positiva.

Acknowledgments

First, I would like to thank my supervisor Cláudia Monteiro, for the availability and knowledge transmitted during this journey, for encouraging my critical thinking and showing me what the investigation world is really like. Secondly, I want to thank Cristina Martins and all the members of the Bioengineered Surfaces group for welcoming me into the group, and help me with any problem that appeared.

Thank you to my co-supervisor, Cláudia Pinho, for all the help and for the hours in front of the confocal microscope. A special thanks to Filipa Soares for guiding me around the lab, and helping me with the experimental work specially after my surgery.

A special thanks to my close friends that have been with me all these years, for always believing in me and motivate me to do better.

Also, to my parents, for the unconditional support, and keeping me in line, they are the real reason for me being where I am today.

This work had the financial support of AntINFECT: Bioengineered Advanced Therapies for Problematic Infected Wounds (POCI-01-0145-FEDER- 031781) e da Fundação para a Ciência e Tecnologia (FCT) (UIDB/50006/2020).

Index

List of Figures

List of Tables

Abbreviations and symbols

AC	Alternate current
AMP	Antimicrobial peptide
CD	Circular Dichroism
DOPC	1,2-dioleoyl-sn-glycero-3-phosphatidylcholine
DPPE-NBD	1,2-dipalmitoyl-sn-glycero-3-phosphoethanolamine-N-(7-nitro-2-1,3-benzoxadiazol-4-yl)
FTIR	Fourier-transform infrared
GUVs	Giant Unilamellar Vesicles
ITO	Indium tin oxide
LB	Langmuir-Blodget
LNPs	Loaded Nanoplexes
LPS	Lipopolysaccharides
LS	Langmuir-Schaeffer
LUVs	Large Unilamellar Vesicles
MLVs	Multilamellar Vesicles
mPLGA-FKR560	Methoxy-Poly(ethylene glycol)-b-Poly(lactide-co-glycolide)-FKR560
NPs	Nanoparticles
NTA	Nanoparticle tracking analysis
PC	Phosphatidylcholine
PdI	Polydispersity index
PEG	Polyethylene glycol

PG	Phosphatidylglycerol
PLGA-PEG	Poly(lactide-co-glycolide acid)-polyethylene glycol
PLGA-PEG-Mal	Poly(lactide-co-glycolide)-b-Poly(ethylene glycol)-Maleimide
POPG	1-palmitoyl-2-oleoyl-sn-glycero-3-phosphatidylglycerol
SLBs	Supported lipid bilayers
SUVs	Small Unilamellar Vesicles
TA	Teichoic acids

Chapter 1 - Introduction

1.1. Context and Motivation

In an era where antibiotic-resistant bacteria are rapidly spreading around the world, antimicrobial peptides (AMPs) seem to have the potential to be one of the alternatives to fight these infections. However, AMPs still present several drawbacks when applied *in vivo*, such as low stability, aggregation and proteolytic degradation. Nanotechnology strategies have already proven in multiple studies that when combined with AMPs can overcome some of these challenges, demonstrating that this is a promising direction for bringing AMPs to the market.

Having this in mind, our group, developed AMP grafted poly(lactide-co-glycolide acid)-polyethylene glycol (PLGA-PEG) nanoparticles (NPs) produced by nanoprecipitation, using a mixture of PLGA-PEG and PLGA-PEG-maleimide (PLGA-PEG-Mal) copolymers, which were further grafted to the AMP MSI-78(4-20), modified with a cysteine at the C-terminus (MSI-78(4-20)-Ahx-Cys). Covalent binding allows a homogeneous surface distribution of the AMP and offers protection from proteolytic degradation and aggregation, moreover, grafting as opposed to encapsulation strategies, maintains targeting and selectivity towards bacteria. Grafting MSI-78(4-20) to these NPs, not only maintained AMP antimicrobial activity in standard growth media and simulated wound fluid, but also accelerated killing kinetics at bactericidal concentrations (submitted manuscript). Despite the maintenance of antimicrobial properties, the minimal inhibitory and minimal bactericidal concentrations of the grafted AMP-NPs increased for the Gram-negative *Pseudomonas aeruginosa* (*P. aeruginosa*) when compared to free AMP, while these values were maintained for the Gram-positive *Staphylococcus aureus* (*S. aureus*), possibly due to differences in their membrane composition which most probably leads to differential interactions with the AMP and AMP-NPs.

However, the study of AMP and AMP-NPs interactions with the bacterial membrane is not simple, mainly due to the complex and dynamic structure of the membrane itself. To overcome these challenges, several biomimetic membrane models have been developed to mimic the arrangement of lipids in natural cell membranes while providing very defined and controlled conditions. One of the most used models are liposomes as they resemble the membrane and cytoplasm of the natural cell structure. More specifically giant unilamellar vesicles (GUV) are the most commonly used, as their size is the closest to natural cell membranes being at the same time easily studied by optical microscopy techniques.

1.2 Objectives

The aim of this work was to unravel the mechanisms of action of MSI-78(4-20) when conjugated to PLGA-PEG NPs, using bacterial membrane models mimicking Gram-positive and Gram-negative bacteria. The interaction was studied by confocal microscopy using fluorescently labelled AMP-NPs and fluorescently labelled membrane mimetic models.

To achieve this aim, GUVs resembling Gram-positive and Gram-negative bacterial membranes were produced. For Gram-positive mimicking GUVs, 1,2-dioleoyl-*sn*-glycero-3-phosphatidylcholine (DOPC) and 1-palmitoyl-2-oleoyl-*sn*-glycero-3-phosphatidylglycerol (POPG) were used, while a mixture of DOPC, POPG, and lipopolysaccharide (LPS) was used for GUVs resembling Gram-negative bacterial membranes. GUVs were produced through an electroformation process and containing 1,2-dipalmitoyl-*sn*-glycero-3-phosphoethanolamine-N-(7-nitro-2-1,3-benzoxadiazol-4-yl) (DPPE-NBD) (green fluorescent probe). Then, fluorescently labelled AMP-NPs were produced and characterized. PLGA-PEG NPs were made by nanoprecipitation of the co-polymers Methoxy-Poly(ethylene glycol)-Poly(lactide-co-glycolide) (PLGA-PEG), Poly(lactide-co-glycolide)-b-Poly(ethylene glycol)-Maleimide (PLGA-PEG-Mal) and Methoxy-Poly(ethylene glycol)-b-Poly(lactide-co-glycolide)-FKR560 (mPLGA-PEG-FKR560) (red fluorescent probe). The AMP MSI-78 (4-20) was further grafted to the NPs through a thiol-maleimide Michael addition reaction.

Chapter 2 - Literature Review

2.1. Antimicrobial Resistance

The phenomenon of resistance was first discovered around the late 1940s when Mary Barber, one of the pioneers in this field, found that bacteria could gain resistance to antibiotics through natural selection, showing the existence of penicillin-resistant strains of *S. aureus*. This happens when bacteria are in the presence of sublethal concentrations of antibiotics, allowing the selection of resistant mutants. These mutations can translate into a series of alterations in different mechanisms, like enzymatic destruction or modification of an antibiotic, increased efflux or reduced influx, or modification of the drug target, which can induce changes in a way that the antibiotics no longer work on the bacteria, making infections harder to treat and increasing the risk of disease spread, severe illness, and death [1].

When the phenomenon of resistance was discovered, it was believed that this transmission would only happen through vertical inheritance to descendent bacteria, but in the 1960s it was discovered that bacterial resistance could also happen through horizontal gene transfer, allowing other microbial species to acquire new genetic material from outside their clonal lineage, through mobile genetic elements that would eventually come to be known as plasmids [2]. The overuse of antibiotics in humans, animals and agriculture leads to a dramatic increase in the widespread of antibiotic resistance.

The era of antibiotics began in the early 1940s with the clinical use of penicillin, and although the risks of antibiotic-resistant bacteria were already known, it wasn't until the late 70s that it started to be considered a threat to global health, that could take humanity to pre-antibiotic times. One of the main events that brought attention to this problem took place in January of 1981, when Stuart Levy, a clinician-scientist, convened a conference where 147 scientists from 27 countries signed a joint "Statement Regarding Worldwide Antibiotic Misuse", which later led to the formation of the "Alliance for the Prudent Use of Antibiotics" [3]. Since then, other steps have been taken to solve this problem, the major ones by the World Health Organization, such as the creation of a "Global Action Plan on Antimicrobial Resistance", with the aim to raise awareness on the health and socioeconomic problems that antibiotic resistance can cause and strengthen research on novel antimicrobial agents. Moreover, this plan aimed at the creation of "The Global Antimicrobial Resistance Surveillance System", where the latest data related to antimicrobial resistance on a global scale is shared [4 - 5].

Accordingly, to a 2019 report from the United Nations antimicrobial resistance causes at least 700,000 deaths globally per year, and, if no action is taken to regulate the use of antibiotics in all sectors and to invest in research and development of new technologies to combat antimicrobial resistance, this number could increase to 10 million deaths globally per year by 2050 [6]. In addition, the increase of infections by antimicrobial-resistance pathogens also places a burden on healthcare systems and has important global economic costs.

In the past years, experts have begun to refer to a group of pathogens as "ESKAPE pathogens", which is an acronym for *Enterococcus faecium, Staphylococcus aureus, Klebsiella pneumoniae, Acinetobacter baumannii, Pseudomonas aeruginosa*, and *Enterobacter* species. These bacteria are characterized by the development of resistance mechanisms against several antibiotics and are common causes of life-threatening infections around the world. For those reasons, they were designated priority status in the 2017 "Global Priority List of Antibiotic-Resistant Bacteria to Guide Research, Discovery, and Development" published by the World Health Organization [7 - 8].

2.2. Antimicrobial Peptides (AMPs)

2.2.1. Background and Structure

The first step towards the discovery of antimicrobial peptides (AMPs) was in 1939 when Dubos extracted an antimicrobial agent from a soil Bacillus strain and proved that it had the capacity of lysing Gram-positive microbial species [9]. The AMP was discovered later in a fraction of this extract and was named gramicidin. In the following years other AMPs were discovered, first, in prokaryotes, and in the 1950's also in eukaryote organisms [10].

Since then, as it is showed in figure 2.1, publications around this topic have increased substantially, more than 5000 AMPs have already been discovered or synthesized, and they have been found in all forms of life like animals, plants, fungi, protozoa, and bacteria [11]. However, there are some key differences, between eukaryotic AMPs, and bacterial AMPs. In eukaryotic organisms, AMPs are considered to be part of the innate immune system and act as the first line of defence, so they can target a large diversity of bacteria. Bacterial AMPs, often referred to as bacteriocins, are much more potent, acting at pico to nanomolar concentrations, as opposed to the eukaryotic AMPs which need micromolar concentrations. Besides that, bacterial AMPs have more specific targets, killing only bacteria closely related to the producer, which gives the producer a competitive advantage against other bacteria, fighting for the same resources [12]. Alongside the increase in the study of this type of molecules, there was a growing interest in the modification of natural derived AMPs, as chemical synthesis of these molecules can have lower costs and improve several aspects of the natural AMPs, like extending their half-life, increasing their resistance to degradation and decrease cytotoxicity.

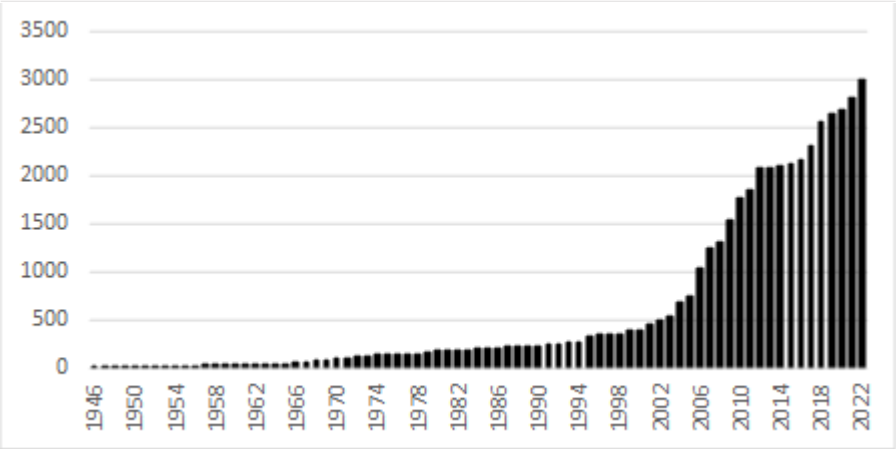

Figure 2. 1 - Number of published papers per year using the search words "antimicrobial peptides" according to PubMed [13].

Regarding structure, AMPs are oligopeptides with lengths that can vary between 5 and 100 amino acids in a linear or cyclic arrangement. In general, AMPs are rich in cationic amino acids, which gives them an overall positive charge, and present an amphipathic structure, due to the presence of hydrophobic and hydrophilic residues. This structure can either be rigid or formed through conformational changes when interacting with bacterial cell membranes [14]. AMPs are also classified based on their secondary structure, the majority of them being ß-sheet and α-helix, although some present an extended/random-coil structure. ß-sheet AMPs are stabilized by disulphide bonds, which confers them a very rigid structure, and are organized in an amphipathic molecule. Defensins, AMPs produced as inactive precursors in neutrophils, macrophages, and epithelial cells, are one of the most studied peptides with this structure. In contrast to ß-sheet peptides, α-helix AMPs do not present a rigid structure and are unstructured in aqueous solution, adopting an amphipathic structure only when in contact with a biological membrane. LL-37 is one of the most studied peptides with this structure and is produced as an inactive precursor in a human cathelicidin antimicrobial protein, present in neutrophils and epithelial cells. Lastly, a minority of AMPs present an extended/random-coil structure that does not have a secondary structure, this type of AMPs folds into an amphipathic structure when in contact with membranes similarly to α-helix peptides. One of the most well-known peptides of this group is indolicidin, produced by bovine leukocytes [15 - 16].

2.2.2. Mechanism of Action

It is generally accepted that the interaction of AMPs with bacterial membranes is correlated with their activity, however, there is still little information about the actual mechanisms of bacterial killing.

It is also recognized that their main mechanism is based on the disruption of the physical integrity of membranes with the formation of pores, presenting selective toxicity that is crucial, to not damage the cells of the host tissue. Electrostatic forces seem to be an important factor in this selectivity [17].

Eukaryotic and bacterial cell membranes have significant differences in their lipid composition. The cytoplasmatic membranes of both Gram-positive and Gram-negative bacteria are rich in negatively charged phospholipids like phosphatidylglycerol (PG), cardiolipin (Cl), and phosphatidylserine. Additionally, the cell wall of Gram-positive bacteria has teichoic acids (TA) in its composition and the outer membrane of Gram-negative bacteria is composed of lipopolysaccharides (LPS), which provide extra electronegative charge to the bacterial surface [17 - 18].

LPS are amphiphilic molecules that play a fundamental role in the formation and function of the outer membrane, contributing to its low permeability and antibiotic resistance and it is composed of three structural domains. The lipid A, which is the hydrophobic portion of the molecule and has very little structural variations between different bacteria, covalently linked to it is a core oligosaccharide, and attached to this a hydrophilic extended polysaccharide referred to as O-antigen. These three domains have variations between species, however, the most diverse component is the O-antigen, which not only vary in structure and composition but, in some bacteria, it is not even present. In such cases, the LPS is commonly referred as rough, as opposed to smooth when the O-antigen is present in the composition [19 - 20].

In contrast, mammalian cell membranes are rich in neutral-charged zwitterionic phospholipids, such as phosphatidylethanolamine, phosphatidylcholine (PC), and sphingomyelin. Furthermore, the zwitterionic phospholipids are in an asymmetric distribution, where all of them are encountered in the outer leaflet, meaning that if any negatively charged phospholipid is present, it will be in the inner leaflet, facing the cytoplasm, also there is a high content of cholesterol which contributes to the membrane stabilization [18].

All the features mentioned above may explain the selective interaction of cationic AMPs towards bacterial membranes, where electrostatic and hydrophobic forces have a role. As opposed to interactions with eukaryotic cells where hydrophobic interactions are prevalent.

After the initial electrostatic interaction, the AMPs are in contact with the cell wall of the bacteria, which they need to overcome to interact with the cytoplasmic membrane. In Gram-negative bacteria, a model termed self-promoted uptake was proposed [21]. According to this model, the AMPs displace de divalent cations (Ca^{2+} and Mg^{2+}) present in the outer membrane that bind to the phosphate groups in the inner core of LPS, this will destabilize the supramolecular assembly permeabilizing the outer membrane, thereby permitting passage of AMPs across the membrane [22]. However, in Gram-positive bacteria, this model does not apply, since instead of LPS, AMPs face a thicker peptidoglycan layer, negatively charged due to the presence of teichoic and teichuronic acids, which seem to be explored by the cationic peptides for permeabilization.

After reaching the cytoplasmic membrane, AMPs will form an amphipathic secondary structure, if they do not possess it already, and they will start interacting with the membrane in two ways, by electrostatic forces between the charged domains of the peptide and head groups of the phospholipids, and also by hydrophobic interactions between domains of the peptide with this characteristic and the core of the lipid bilayer, leading to an accumulation and insertion of the AMPs in the membrane [18].

Although it is widely accepted that this will cause the formation of pores, leading to the disruption of the ion flow across the membrane, and ultimately causing cell death, the process of how this happens is still subject of discussion, and several models have been proposed. The three main models are: the barrel-stave model, which states that as the peptides accumulate in the membrane, they will start to insert perpendicularly in the bilayer to form a peptide-lined transmembrane pore, with the hydrophobic domains interacting with the core of the bilayer and the hydrophilic domains oriented to the aqueous channel of the pore; the toroidal-pore model, states that the peptides also insert perpendicularly and this will force the membrane to bend resulting in a pore lined by both peptides and head groups of phospholipids, this kind of pore is unstable and can force some peptides into the intercellular space upon disintegration; finally the carpet model, in this model there is no formation of pores, instead, the peptides accumulate parallel to the membrane and, after reaching a threshold density of coverage, the tension caused in the membrane leads to its disruption and production of micelles in a detergent-like effect [23]. A representation of these models can be found in figure 2.2.

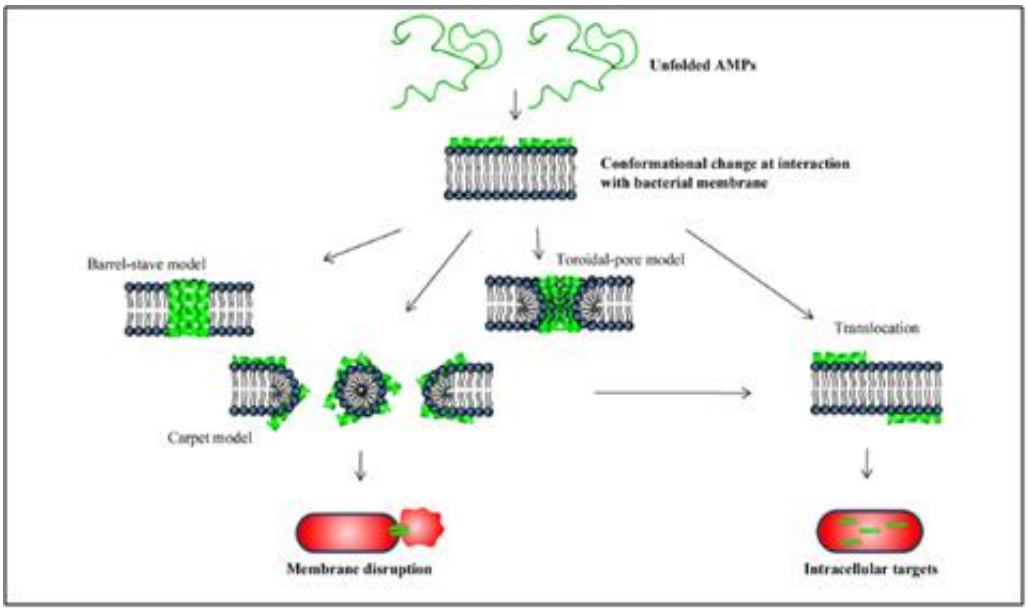

Figure 2. 2 - Schematic illustration of bacterial killing mechanisms by AMPs [14].

It has also been shown that some AMPs have other mechanisms of action which allows them to translocate into the cytoplasm to find non-membrane targets blocking essential cellular processes like DNA/RNA and protein synthesis, protein folding, enzymatic activity, cell wall synthesis, or even cause activation of autolysins [24].

Besides direct microbicidal activity, AMPs can also have immunomodulatory activity which leads to an effective bacterial clearance by the host. This immunomodulatory response acts through various mechanisms like, stimulation of chemotaxis, initiation of adaptive immunity and modulation of immune cells like the activation and recruiting of lymphocytes. Other mechanisms include the production of proinflammatory cytokines, anti-endotoxin activity and suppression of toll-like receptors [25].

2.2.3. Resistance

Regarding AMP resistance development, the current views suggest that the mode of action of AMPs minimizes the probability of bacteria to develop resistance as it mostly targets the negatively-charged membrane of bacteria, making it a very unspecific mechanism when compared to conventional antibiotics that have just one high-affinity target, mostly enzymatic. So, to develop resistance, bacteria would have to redesign their membrane lipid composition while preserving its functionality and structural integrity, which is relatively difficult to accomplish [26].

However, a variety of studies have recently emerged describing some resistance mechanisms that bacteria developed when in the presence of AMPs, and these can be divided into intrinsic and acquired resistance. Intrinsic resistance mainly happens through the incorporation of positively charged molecules into the bacterial surfaces, reducing the binding affinity with AMPs. For Gram-Negative bacteria these modifications happen in the LPS, for example, in *Salmonella Typhimurium* (*S. Typhimurium*) the addition of the positively charged 4-aminoarabinose to lipid A, a component of the LPS was observed [27]. As for Gram-Positive bacteria, modifications happen in TA of the cell wall. In *S. aureus* resistance is induced by several mechanisms when in the presence of AMPs, like D-alanylation of TA and the incorporation of lysylphosphatidylglycerol in the bacterial membrane [28]. Besides, other intrinsic resistance methods have been described, as the removal of AMPs by efflux pumps or proteolytic degradation. These phenomena happen both in *S. Typhimurium* with the sap (sensitivity to antimicrobial peptides) efflux system, which exports AMP from the cells, and the production of PgtE protease that has the ability to degrade AMPs [27 - 28].

Acquired resistance happens when bacteria develop resistance to an agent that they were susceptible to, this mainly happens through mutations or acquisition of foreign genetic material. Studies to access if bacteria can acquire resistance to AMPs have already been done *in vitro* for some pathogens through isolation of naturally occurring resistant isolates, by serial passage in the presence of AMPs, and direct plating with AMPs. Some examples are the rise of resistance in *Escherichia coli* and *Pseudomonas fluorescens* after continuous exposure to gradually increasing concentrations of pexiganan, an analogue of the naturally occurring mangainin 2 [31]. Or the naturally occurring small colony variants in *S. aureus* which have been associated to resistance to several AMPs, due to reduced metabolic activity and diminished transmembrane potential [32].

Nevertheless, among the existing antibiotic alternatives, AMPs arise as one of the most promising alternatives regarding risk of resistance development.

2.2.4. AMPs in pre-clinical and clinical investigation

As up today, the data repository of antimicrobial peptides contains 5891 AMPs, from natural and synthetic origin, of which 77 are currently in preclinical or clinical stage and only a minority has obtained food and drug administration (FDA) approval. Some of the reasons for this failure include toxicity of the AMPs toward mammalian cells and poor stability, which translates into a shorter half-life [33]. In fact, only 7 AMPs have received FDA approval, namely,

gramicidin D, daptomycin, vancomycin, oritavancin, dalbavancin, telavancin, and colistin, all of them are bacteriocins discovered in or derived from Gram-positive bacteria. They are composed of several noncanonical amino acids and have chemical modifications or cyclic structures which extend their half-life and, as the majority of AMPs, they are used for treating Gram-positive bacterial infections [34].

Even though AMPs have potent activity *in vitro*, the *in vivo* activity is, most of the times, much lower because of the complexity of the physiological environment, which affects their stability and efficacy. Consequently, several AMPs that enter drug development failed during their clinical phases. Pexiganan was one of the first AMPs evaluated for the treatment of infected wounds, it was shown to promote dermal cell migration and antibacterial activity against Gram-positive and Gram-negative bacteria in diabetic foot ulcer models, but it ended up failing during phase III due to lack of efficacy compared to other antibiotics [35]. Other examples of AMPs that failed in phase III are iseganan, which objective was to prevent polymicrobial oral infections, XMP-629 to treat impetigo and acne rosacea, murepavadin to treat ventilator-associated bacterial pneumonia, all of them due to lack of efficacy or to multiple side effects [34]. Even so, there are some promising results about some AMPs, one of the most well-known is the cathelicidin LL-37, which is in phase II of clinical trials and is meant to be used in the treatment of diabetic foot ulcers. LL-37 leads to membrane disruption through the formation of pores, following the toroidal-pore model, and it was shown to promote angiogenesis, migration, and proliferation of dermal cells, however, more clinical studies are needed to determine its efficacy and potential side effects [35]. Other examples of AMPs in phase II clinical trials with promising results are, LTX-109, a synthetic peptide being tested for the topical treatment of impetigo and nasal decolonization of methicillin-resistant *S. aureus*, which induces pore formation in bacterial membranes with a MIC range of only 2-4 μg/mL against Gram-positive bacteria. And DPK-060, a peptide derived from the endogenous human protein kininogen, being tested for the treatment of acute external otitis and atopic dermatitis, has proved to treat a broad range of infections, including Gram-negative bacteria and fungi, through membrane disruption, as well as immunomodulation [36].

2.2.5. Strategies to Improve AMPs Effectiveness

As mentioned, the introduction of AMPs in clinical use faces a lot of challenges. AMPs are not completely selective to microbial cells and can be toxic for eukaryotic cells as well, they are chemically unstable, which limits oral and intravenous administration due to their rapid degradation by proteolytic enzymes and they penetrate poorly the intestinal mucosa, limiting bioavailability even further. Also, AMPs present large discrepancies between *in vitro* and *in vivo* activities, due to their high sensitivity to environmental conditions and production costs are much higher when compared to conventional antibiotics [37].

Currently, several methods have been tested to overcome these drawbacks, some examples of modifications of the AMPs are the production of ultra-short or truncated AMPs, which has been pursued by several companies to reduce production costs, and consists in reducing the amino acids of the “original” peptide without losing its main characteristics. Covalent coupling with polymers is another very used technique once these materials are already widely used for medical applications, polyethylene glycol (PEG) is one of the most used polymers for this purpose. This functionalization, named PEGylation, has shown many evidences

that it can increase resistance to degradation, reduce aggregation and toxicity toward mammalian cells. Several features of the AMPs play an important role in the bactericidal activity and toxicity, such as the α-helical content, hydrophobicity, net charge and others which can be tuned through chemical modifications of the peptides. Proteolytic stability has been increased through different approaches like the introduction of D-amino acids, cyclization, amidation or acetylation of the terminal regions [38].

Besides AMP modifications, during the last decades, many studies have been done to find novel forms for peptide delivery. One of these strategies is the incorporation of AMPs into polymeric scaffolds such as hydrogels. These have great potential in wound dressing and several other biomedical applications due to their ability to retain high amounts of water or biological fluids within their network, promote cell attachment and proliferation, and extracellular matrix regeneration. There are several ways to incorporate the AMPs into hydrogels, such as simply mixing them with the polymer or using the AMPs to promote charged interactions with the polymers leading to the hydrogel formation, among others. This incorporation can bring many advantages. First, the peptides inside the polymeric network are more protected from enzymatic degradation, and, second, the high-water content protects the peptides from denaturation. Lastly, it is possible to tune the polymers, by changing several parameters like the degree of cross-linking, chemical structure of monomers, or its concentration, in order to have a controlled and targeted release of the peptide and achieve effective therapy [39]. One example of this technique is Granexin, a hydroxyethyl cellulose hydrogel incorporated with ACT1 AMP, with the goal of treating diabetic foot ulcers. In the III clinical trial, Granexin proved to be safe and effective with a reduction in the ulcer area superior to the control, and in a short time, all the patients reached full re-epithelization of the ulcer [40].

Another area that has emerged in the past years and seems to have great potential for peptide delivery is nanotechnology. This field studies the phenomena taking place in the nanometric scale, between 1 and 100 nm, with the purpose of designing and producing systems in that scale, which unravels a variety of different possibilities in several areas, especially biomedicine. Usually, these systems have a high surface area to volume ratio, making them great to use as drug delivery systems, also called nanocarriers. The simple conjugation of AMPs with nanocarriers seems to overcome some of the main challenges mentioned above, as it can physically protect AMPs against degradation in different environments and reduce its toxicity towards the host cells.

AMPs conjugation can be obtained by two main methods, loading of the AMPs into the nanoparticles and surface immobilization. Since the mechanism of action varies between the AMPs, the conjugation method must be in accordance with it, for example, for AMPs that interact with intracellular targets, drug loading may be the most adequate. In this case, the AMPs need to penetrate the bacterial membrane to induce their effect, and NPs are most of the times taken up by the microorganism, having an adequate release rate, the AMP will only be released intracellularly, increasing its antibacterial effect. On the other hand, this method would not function so well with AMPs that interact with the bacterial membrane, because they would need to be released outside the bacteria, hence surface immobilization may be more adequate since it allows the AMP to directly interact with the bacterial membrane, leading to a faster antimicrobial activity, not dependent on the release rate [41].

Furthermore, since these systems can be made from several different biocompatible materials, such as polymers, lipids, and metals, it is possible to tune the physicochemical properties of the materials to develop system-specific features. These have even greater advantages, like a controlled release of the AMP towards a specific organ, a better pharmacokinetic profile, the ability to be environmentally responsive, minimize side effects, and an overall increase in therapeutic efficacy [42].

Besides enhancing the AMPs bactericidal efficacy, there have been several studies that demonstrated that various nanoparticles have intrinsic antibacterial properties against both Gram-positive and Gram-negative bacteria. Even though the mechanisms have not been thoroughly explained, there are three main reasons for their antibacterial effect: oxidative stress induction, metal ion release, which occur in metallic nanoparticles, and other non-oxidative mechanisms like penetration and disruption of the bacterial cell membrane and interaction with DNA and proteins [43].

2.2.5.1 Poly(lactic-co-glycolic acid) and Polyethylene glycol

One of the synthetic polymers with most success in drug delivery is poly(lactic-co-glycolic acid) (PLGA). This polymer is hydrophobic and, when in contact with water, it degrades into lactic acid and glycolic acid, two monomers that are already produced by the human body and are easily metabolized via the Krebs cycle, which makes it non-toxic and biodegradable. Another advantage of this polymer Is his tunability, as properties like its mechanical strength and degradation rate can be adjusted for specific applications, by changing parameters like its initial molecular weight and the ratio of lactic acid and glycolic acid monomers [44].

However, the body recognises hydrophobic particles, like PLGA, as foreign and eliminates them by phagocytosis or by taking them up to liver or spleen. To address this problem several surface modifications of PLGA have been tested, in order to hide its hydrophobicity. One of the most promising is a modification referred before, the PEGylation. Polyethylene glycol (PEG) is commonly classified as a “stealth polymer” due to its hydrophilic, non-ionic and inert character, which confers great biocompatibility and absence of activate and aggressive response from the body [45].

So, by using an amphiphilic copolymer with a hydrophobic chain, like PLGA, and a hydrophilic one, like PEG, it is possible to create nanoparticles where the PLGA is surrounded by PEG and with this increase its circulation or residence time [46].

2.2.5.2. MSI-78(4-20)

The AMP MSI-78, commercially known as pexiganan, was initially designed to treat infected diabetic foot ulcers, it has broad-spectrum of activity being effective against both Gram-positive and Gram-negative bacteria through the disruption of the bacterial membrane via toroidal-type pore formation [47].

Having various studies reported that the length of the AMP relates with its cytotoxicity, and its production costs, our group designed six 17-mer peptide sequences based on the

sequence of MSI-78 (22-mer), by spanning the whole sequence of MSI-78 (4-20) by one aminoacidic shift. Antimicrobial activity was tested against *S. aureus*, *Staphylococcus epidermidis*, and *P. aeruginosa*, revealing that one of the short derivatives, MSI-78 (4-20), was as effective as the parent peptide while it reduced hemolytic activity against human red blood cells [47].

In comparison with the original peptide, the MSI-78 (4-20) presents a lower net-charge, a higher hydrophobicity, and a lower percentage of helicity. Although the higher net-charge of the MSI-78 favours the electrostatic interactions with the bacterial membrane, the higher hydrophobicity of the MSI-78 (4-20) may lead to a deeper insertion into the lipidic bilayer which can explain their similar effectiveness [47].

The interactions of MSI-78(4-20) with bacterial and eukaryotic cells were also studied with the help of two biomembrane model systems, specifically using large unilamellar vesicles (LUVs), one composed of 1,2-dimyristoyl-*sn*-glycerophosphocholine (DMPC) to mimic the mammalian membrane, and the other by a mixture of 1-palmitoyl-2-oleoyl-*sn*-glycero-3-phosphocholine (POPC) and 1-palmitoyl-2-oleoyl-*sn*-glycero-3-phosphatidylglycerol (POPG) at a 1:1 molar ratio to mimic the bacterial membrane. The interaction was evaluated based on the variations of the zeta potential (ZP) and hydrodynamic diameter (HD) of the models, as expected the ZP and HD of the DMPC models did not vary with the addition of the AMP, while there was a concentration-dependent increase in both parameters for the POPC:POPG models, suggesting the selectivity of the AMP towards bacterial membranes [47]. Circular dichroism analysis revealed that both the parent peptide and the MSI-78(4-20) presented random coil conformations in aqueous buffer and in the presence of the DMPC LUVs, however, when in the presence of the POPC:POPG LUVs, they both presented α-helical conformations, which confirmed their selectivity towards bacterial membranes [47].

2.3. Bacterial Membrane Mimetic Models

Currently, evidence has shown that antimicrobial drug molecules present in the market, with diverse chemical structures and several therapeutic effects, indirectly interact with the bacterial membrane, namely with the proteins, such as G protein-coupled receptors, leading to changes in drug physicochemical properties, pharmacological activity, and bioavailability [48]. Also, a lot of the new drugs have as their main target the bacterial membrane, like most of the AMPs. This focus on the bacterial membrane is not random, as the lipids that compose the membrane maintain its structure and the biological activities of the proteins, and also play important roles in several cellular activities such as cell adhesion and cell signalling, which makes them a great target for therapeutic action. On the other hand, if the interaction with the membrane does not work, it can have adverse effects, such as drug resistance and severe side effects due to low drug specificity, so, it is of great importance that these interactions drug-membrane are carefully studied [48].

Although it is possible to study the interaction between drugs and bacterial membranes using the bacteria itself, this is not as easy as it seems, mainly because the membrane is a very complex structure with a polymorphic lipid arrangement and a variety of lipids that change between species, each one with different physical properties [49]. These dynamic characteristics make the study of a specific interaction very difficult to analyse, as well as,

very expensive since it requires superior installations and specialized professionals. To overcome these challenges, several biomimetic membrane models have been developed to mimic the arrangement of lipids in natural cell membranes in very defined and controlled conditions, allowing to study the role of individual components [50].

Among the several models that exist, the most used ones are Langmuir monolayers, supported lipid bilayers (SLBs), and liposomes (figure 2.3). Choosing an adequate model depends deeply on the objective of the study since each one has certain advantages and disadvantages.

Langmuir monolayers, also referred to as lipid monolayers, are the simplest model of the three and yet very useful. They can be formed by spreading amphiphilic lipids at an air-water interface, which leads the lipids to organize into a monolayer. Having a monolayer instead of a bilayer brings some advantages, parameters such as lipid composition, subphase and temperature can be chosen to mimic biological conditions without any limitations, they are very stable and well-defined and the exact geometry can be determined [51].

Given the characteristics of this model, it allows a detailed investigation of drugs interaction with lipid head groups, through several methods like the surface pressure of the monolayer or Brewster angle microscopy [52]. For example, this has been used to evaluate the penetration of numerous AMPs, like melittin and defensin A, through various phospholipid compositions [53]. However, this is a very simplistic model that does not reflect the complexity of biological membrane structure.

SLBs are stable planar bilayer structures adhered to a solid support, which enables one of the leaflets exposures to buffered solutions. There are three main techniques to prepare them, a direct fusion of lipid vesicles onto the solid supports, the Langmuir-Blodget (LB) technique, or a combination of the LB with the Langmuir-Schaeffer (LS) techniques, which can be done in different substrates such as silica, mica, metal, and others [49]. In the LB, a substrate previously immersed is vertically lifted through a Langmuir monolayer which is transferred into the substrate. This substrate is then dipped vertically into another Langmuir monolayer forming a lipid bilayer. In the combination of LB and LS techniques, a monolayer is transferred to the substrate through the LB technique but instead of dipping it, the second monolayer is transferred by getting the substrate in contact with a monolayer with parallel orientation.

This type of model offers high bilayer stability while maintaining the mobility of the lipid molecules which makes it suitable for studying drug-membrane interactions. Besides, it is possible to analyse it through a variety of different techniques like scanning and transmission electron microscopy, atomic force microscopy, quartz crystal microbalance with dissipation among others [54].

Finally, there are liposomes, which are spherical lipidic vesicles composed of two or more lipid bilayers, with an aqueous core. They are one of the most used models because they resemble the membrane and cytoplasm of the natural cell structure and are also relatively easy to prepare and handle. Depending on their size and structure, the liposomes can be divided into small unilamellar vesicles (SUVs), large unilamellar vesicles (LUVs), giant unilamellar vesicles (GUVs), and multilamellar vesicles (MLVs). These can be produced by numerous

methods that have been developed over the years, namely thin-film hydration, sonication, electroformation, swelling, ink-jet injection among others [55].

Since its structure is a simplified version of a natural cell membrane, this makes them very useful to study the interaction and permeability of drugs or drug delivery systems with membranes of different compositions. A variety of different methods to study these interactions has been described, such as the evaluation of the interaction of ionized compounds with biomembranes using liposome/water partitioning systems, the use of immobilized liposomes as the stationary phase in chromatography to achieve a rapid screening of drug partition in lipid bilayers, and also the use of different microscopic and spectroscopic techniques to evaluate the contribution of these biophysical interactions to the efficacy of drugs [48].

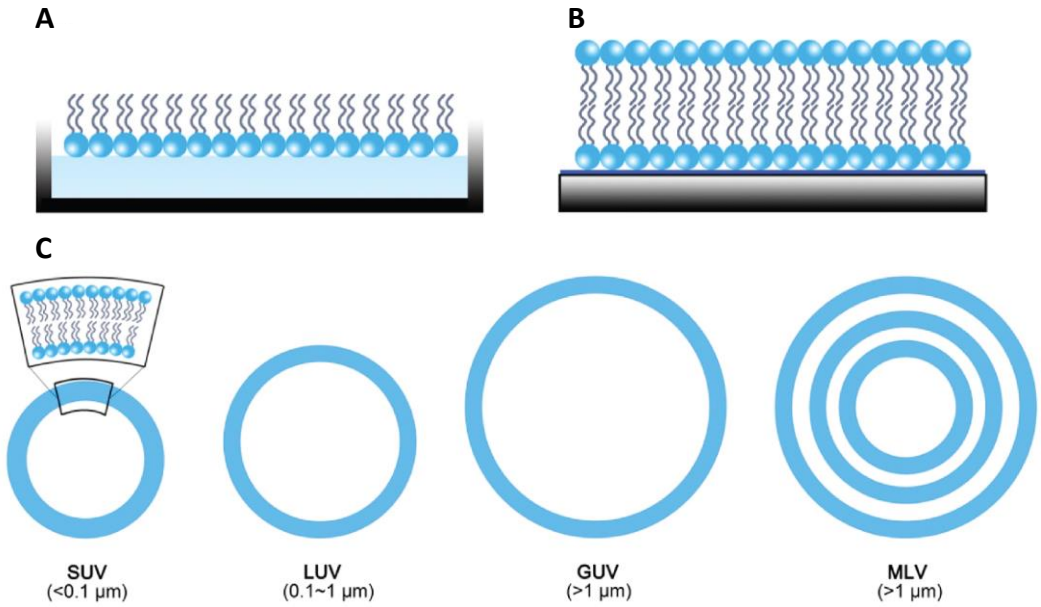

Figure 2. 3 - Schematic representation of a Langmuir monolayer (A), a supported lipid bilayer (B) and liposomes classified according to their size and number of bilayers (C) [46].

2.3.1. Giant Unilamellar Vesicles

From the different types of liposomes, GUVs are the ones that have been more used to study membrane biophysics during the past years. This is due to their size, between 1µm and 100µm, being the closest to natural cell membranes and also detectable by optical microscope techniques.

This type of liposome began to appear during the late sixties, and its preparation process was first described by Reeves and Dowben, by a process referred to as gentle hydration or spontaneous swelling which is still used nowadays in the preparation of GUVs [56]. Since then, this process suffered several improvements, and other processes have been developed and GUVs that were initially used to study the properties of bilayers now have much more applications.

2.3.1.1. Preparation Processes

As mentioned, Reeves and Dowben demonstrated GUVs formation through gentle and slow hydration of a dried lipidic film. This was done by preparing a lipidic solution in an organic solvent, like methanol or chloroform, and spreading it on a glass substrate. After the evaporation of the solvent the hydration starts, with either water or an aqueous solution of non-electrolytes, such as sucrose [56]. The main factors contributing to GUVs formation seem to be a combination of various aspects such as osmotic pressure, electrostatic interactions, and hydrophobic effects. Since then, different variations have been developed based on the same principles, to improve GUVs features.

However, as with every method, spontaneous swelling has some disadvantages, GUVs preparation needs to be carried out under strict and controlled conditions such as temperature, lipid composition and ionic composition of the surrounding medium, and it takes a long time to complete, normally more than one day. Moreover, production yield is variable and relatively low, and many GUVs present defects, resulting only in a small portion of ideal GUVs [57].

It has been demonstrated that the addition of different components to the phospholipidic mixture such as 10 - 20 mol% of charged lipids, like phosphatidylserine or phosphatidylglycerol, divalent ions, Ca^{2+} or Mg^{2+}, and sugars, promoted the swelling of the vesicles and increased the yield [53 - 54]. Besides the addition of components, some studies show that different *stimuli* like localized heating and pressure waves have been shown to improve the structural quality of GUVs in different media [57 - 58]. There are also other methods being tested like the use of surfaces with photolithographic templates as substrate, intending to homogenize the size of the GUV population, or the inclusion of photoactive compounds to promote the swelling of the GUVs when irradiated by UV light [59 - 60].

The spontaneous swelling was also the base of the gel-assisted swelling, the improvement in this method was the coating of a glass substrate with a polymer-based gel, this modification adds a buffer influx from below the bilayers. This change in substrate reduces drastically the preparation time, from days to minutes, allows the use of a wider range of lipid compositions and buffer conditions, and seems to have great potential in the encapsulation of biomolecules [63].

This method was first developed with agarose gels and, even though it presented the advantages referred, it was later discovered that some agarose molecules were trapped inside the vesicles during its formation. Although this contamination did not interfere with the molecular mobility of the lipids it led to altered physicochemical properties of GUVs [56]. Different polymers were also tested since then such as chemically crossed-linked polyacrylamide and polyvinyl alcohol, but the first one presented a lower yield and the second presented changes in the membrane properties, a sign of contamination [61 - 62]. In the recent past, a different approach was taken by cross-linking dextran polymers with PEG, which anchors the polymer to the glass surface and prevents it from dissolving. This allows some control of the vesicle size by modulating the degree of cross-linking and supposedly preventing contaminations however, more studies need to be performed to confirm if the membrane properties stay the same [65].

Another method based on the swelling of the vesicles is electroformation, or electroswelling, which was developed by Angelova and Dimitrov in 1986. It is similar to the other swelling processes in the way that it starts with the hydration of a dried lipidic film, but instead of being deposited on glass or gel, this is done on an electrically conductive surface [59]. The most common materials for these conductive surfaces are indium tin oxide (ITO) coated glass and platinum wire. After the lipidic film is created, a swelling solution is added, and another conductive surface is added on top, separated by a non-conductive spacer, an alternate current (AC) is then applied to the surfaces, creating an external electric field that will influence the swelling process [66].

With this method it is possible to obtain a population of relatively homogeneous GUVs, however, this may vary depending on the conditions, so finding the optimal experimental settings is the key to the electroformation process. Finding these conditions is not an easy task as several parameters have to be defined such as temperature, which must be above the transition temperature of all the lipids in the mixture, the thickness of the film, which will depend on the solution itself and its deposition mode, the AC electric field strength which will influence the average size and the size distribution of the GUVs, among others like the duration of the electric pulses, the overall process time and the hydration medium [67]. On the other hand, this makes the technique very versatile allowing the creation of a variety of different vesicles.

Although this process has been described for the first time in the late eighties, the GUVs formation process is not yet fully understood, however, it is believed that the electrical field can create a gentle mechanic agitation that destabilizes the lipids allowing them to reorganize in the form of vesicles [68].

Several protocols have been created as a result of the widespread usage of electroformation, with slight modifications in the parameters based on the desired qualities of the vesicles. Recently, Nanion Technologies has developed the Vesicle Prep Pro, an electroformation device that has not been widely found in scientific literature, but the number of publications is rapidly increasing because of its versatility and practicality.

Figure 2. 4 - Vesicle Prep Pro. Equipment produced by Nanion Technologies for electroformation of GUVs.

Besides the methods based on the swelling of the vesicles, other methods have been appearing during the last decades. One of them is the droplet transfer method, this has gained a lot of interest because it allows the preparation of vesicles with different inner and outer solutions, an essential step towards the formation of synthetic cells. This is achieved by firstly adding water droplets to a lipidic solution, which leads to the formation of a monolayer around the droplet, secondly, this solution is added to an oil solution with a monolayer on its surface, the weight of the droplets will lead to sedimentation pulling the lipids of the second monolayer in the process and forming the bilayer [69]. Even more recently, with the emergence of microfluidics, some novel approaches have been developed to automatize this process.

2.3.1.2. Applications

Due to the unique characteristics of GUVs, namely their biocompatibility, the ability to conjugate lipophilic and polymeric molecules in their membrane, and its cell-mimicking characteristics, GUVs are a very versatile tool that can be applied in several different contexts. For example, they are being studied as technologies in the medical and pharmaceutical context, as biosensors, in the study of the membrane physicochemical characteristics in different contexts, and GUVs seem to have also great potential in the field of artificial cell synthesis [70].

Probably one of the most interesting, and also more complex applications of GUVs, is the development of an artificial cell. Although the interior of a cell is of extreme complexity and singularity, some steps have been taken to make GUVs more similar to actual living cells. One essential step for this objective is the expression of proteins inside the vesicle since they regulate the activity of the cells, as well as their communication with the environment. This was done by some groups, for example, Saito et. al entrapped a plasmid coding for a green fluorescent protein along with the transcription-translation kit inside giant vesicles, and observed the protein expression with this system [71]. Another important aspect is the reconstitution of the cytoskeleton of the cell, and some promising steps have also been taken in this direction, with the encapsulation of the proteins necessary for its construction into the GUVs. For example, the encapsulation of F-action and meromyosin resulted in the formation of actin filaments, that were later anchored in the inner layer of the GUVs membrane [69 - 70].

Biosensors are another area that has been exploring the potential of GUVs. This type of research is still in the early stage, but there seem to be two main approaches to their utilization. The encapsulation of fluorescent-marker molecules to detect the presence of bacteria producing lysins, and the other approach is to graft receptor molecules in their surface, like antigens or antibodies, to be used as immunoassays [71 - 72].

However, GUVs main application is the study of the membrane in different environments and its interaction with different molecules. There are some clear advantages in using GUVs instead of smaller liposomes, such as the possibility of performing direct visualization and quantitative analysis of pore formation in phospholipid membranes, which was performed with the peptide magainin-2 [75]. This was possible as giant vesicles allow the observation of reactions occurring on the surface of the vesicles and details of fusion and fission of the membrane, which does not happen with smaller vesicles like LUVs or SUVs. GUVs have

also been crucial to study membrane proteins, since the discovery of methods that allowed the incorporation of proteins into the bilayer like the detergent depletion method [76].

When the aim is to mimic the cell membrane of a certain species, the lipidic composition is very important as it varies from specie to specie. As referred before, there are some key differences in the composition of eukaryotic and bacterial membranes. So, from a biological point of view, since PCs are practically absent in bacterial membranes and are the most abundant phospholipid in eukaryotic membranes, a zwitterionic lipid containing PC is normally used to produce eukaryotic mimetic membranes. The opposite happens with PGs, as they are absent in eukaryotic membranes but are ubiquitous in bacterial membranes, which makes the use of negative charged lipids containing PGs adequate to produce bacterial mimetic membranes [75 - 76]. Between the bacterial membranes the objective is them to distinguish the Gram-Positive from the Gram-Negative membranes, with that objective, normally LPS is incorporated in the lipidic composition of the Gram-Negative GUVs, as they are only present in this type of bacteria [79].

Following, there are some examples of GUVs used for interaction studies. Pedro Costa, studied the anti-bacterial effect of fusogenic liposomes loaded with superparamagnetic iron oxide nanoparticles against *S. aureus*. In this case, to mimic *S. aureus* membrane, the GUVs were produced by the electroformation of a mixture between 1,2-dioleoyl-*sn*-glycero-3-phosphatidylcholine (DOPC): 1-palmitoyl-2-oleoyl-*sn*-glycero-3-phosphatidylglycerol (POPG) (7:3) ratio and a 0.2 molar percentage of 1,2-dipalmitoyl-*sn*-glycero-3-phosphoethanolamine-N-(7-nitro-2-1,3-benzoxadiazol-4-yl) (DPPE-NBD) to allow the direct observation in a fluorescence microscope. This allowed observation of the fusogenic capacity of the loaded lipossomes with the GUVs membranes, which were promising results for future works [80].

Montis et al. studied the interaction of antimicrobial 12-bis-THA-TFD loaded nanoplexes (LNPs) with Gram-positive and Gram-negative bacterial biomimetic membranes. For this purpose, they proceeded to the electroformation of two different lipid mixtures, 90 % w/w POPC and 10 % w/w Cl for Gram-positive models and added 17 % w/w of LPS to the Gram-negative models. They discovered that the LNPs have a great affinity to the LPS, induce destabilization, and increase the permeability of the membrane, making them an efficient therapy for Gram-negative infections [79].

Chapter 3 – Materials and Methods

3.1 AMP-NP production

3.1.1 NP Production

NPs were produced by nanoprecipitation through a solvent displacement method. First, a mixture of 20 mg of three different solid copolymers, which properties can be found in table 3.1, was dissolved in 1 mL of acetone according to the following percentages: 55% Methoxy Poly(ethylene glycol)-Poly(lactide-co-glycolide) (mPLGA-PEG), 40% Poly(lactide-co-glycolide)-b-Poly(ethylene glycol)-Maleimide (PLGA-PEG-Mal) and 5% Methoxy-Poly(ethylene glycol)-b-Poly(lactide-co-glycolide)-FKR560 (mPEG-PLGA-FKR560, (50:50 LA:GA)) (PolySciTech; Indiana, USA) (table 3.1). mPEG-PLGA-FKR560 contains the fluorescent probe FKR560, which has maximum absorbance at 562 nm and maximum emission at 584 nm. After the dissolution of the polymers, the solution was slowly dispensed into 10 mL of type I ultrapure water (Milli-Q, Merck, Darmstadt, Germany) under agitation (230 rpm) leading to the formation of the NPs and kept agitating for 2 hours to allow the evaporation of acetone.

Meanwhile, Amicon ® Ultra 15 Centrifugal filter units, 100KDa, were sterilized by centrifugation, once with 10 mL of ethanol 70 % (v/v) and twice with 10 mL of type I ultrapure water for 10 minutes at 2500 rpm. After production, the NPs suspension was transferred to the previously sterilized filters and centrifuged for 10 min at 2500 rpm, then the suspension was washed twice with ultrapure water, and a third time in phosphate buffer (pH 6.6), composed of 0.0625 M sodium phosphate dibasic dihydrate ($NaH_2PO_4 \cdot 2H_2O$) and 0.0375 M sodium phosphate monobasic dihydrate (Na_2HPO_4), in type II ultrapure water. Finally, the NPs were collected in 800 µL of phosphate buffer.

3.1.2 AMP Functionalization

The AMP MSI-78(4-20) modified with a cysteine at the C-terminus (MSI-78(4-20)-Ahx-Cys) (table 3.1) was produced by solid-phase peptide synthesis (SPPS) at Paula Gomes Lab (REQUIMTE, Departamento de Química e Bioquímica (DQB), Faculdade de Ciências da

Universidade do Porto (FCUP), Portugal). For functionalization, NPs were mixed with 200 µL of AMP dissolved in phosphate buffer (p 6.6), in a 1:2.5 Mal-AMP molar ratio.

The mixture was left to agitate at 110 rpm at room temperature (rt) overnight in an orbital shaker, allowing AMP grafting through a thiol-maleimide Michael addition reaction between the Maleimide group exposed in the NP and the sulfhydryl of the AMP (figure 3.1). On the following day, NPs were washed three times with type I ultrapure water using sterilized Amicon filters, and finally recovered in 1mL ultrapure water and stored at 4ºC until further use. A representation of the produced NPs can be found in figure 3.2.

Table 3. 1 - Chemical properties of the polymers and peptide used in AMP-NP production.

Identifier	Name	Molecular Weight (Da)
PLGA-PEG	Methoxy poly(ethylene glycol)-b-poly(lactide-co-glycolide)	3000 - 36000
PLGA-PEG-Mal	Poly(lactide-co-glycolide)-b-poly(ethylene glycol)-maleimide	30000 - 5000
mPEG-PLGA-FKR560	Methoxy-Poly(ethylene glycol)-b-Poly(lactide-co-glycolide)-FKR560 copolymers	3000 - 36000
MSI-78 (4-20)	KFLKKAKKFGKAFVKIL-Ahx-Cys	2211

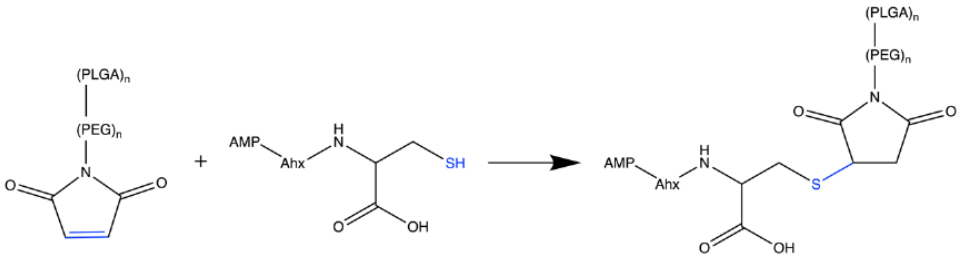

Figure 3. 1 - Representation of the thiol-maleimide reaction between PLGA-PEG-Mal and cysteine-modified MSI-78(4-20) (MSI-78(4-20)-Ahx-Cys).

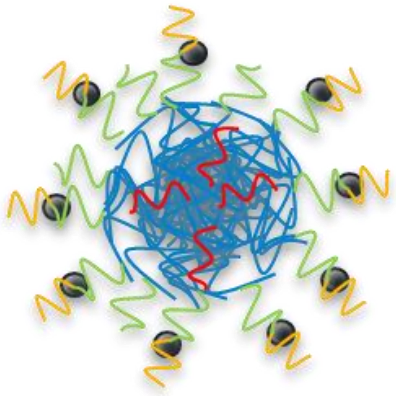

Figure 3. 2 - Representation of the NPs produced. NPs are composed of a mixture of mPEG-PLGA, PLGA-PEG-Mal and mPEG-PLGA-FKR560 copolymers with AMPs covalently immobilized through a maleimide-thiol Michael addition reaction. PLGA is represented as blue, PEG as green, Mal as black, FKR560 probe as red and MSI-78 (4-20)-Ahx-Cys as yellow.

3.2 AMP-NP Characterization

3.2.1 Dynamic and Electrophoretic Light Scattering

The determination of the size and zeta potential of the NPs was performed sequentially in the same equipment, Zetasizer Nano ZS, from Marvern Panalytical, based on the techniques of dynamic and electrophoretic light scattering, respectively. For both techniques, samples are illuminated with a laser and the intensity of the scattered light is detected by a sensitive avalanche photodiode detector. DLS measures the scattered light of the particles in solution, which allows measuring the rate of the Brownian motion, which is correlated with hydrodynamic diameter. In the case of electrophoretic light scattering, movement of charged particles is induced by creating an electric field between two electrodes and through the scattered light it is possible to determine the velocity of the particles and then their zeta potential.

First, the sample was prepared for the test, by diluting the NPs suspension in sodium chloride (NaCl) 10mM, by a dilution factor of 1:100. Then, a disposable folded capillary cell (DTS1070) was prepared by flushing 5 mL of ethanol to facilitate wetting. After, the cell was slowly filled with the NPs sample to avoid the formation of air bubbles.

The following analysis parameters were then defined in the software: For size and zeta analysis: Cell: DTS1070; material: polystyrene latex, with a refractive index of 1.590 and absorption of 0.010; dispersant: NaCl 10mM with 0.8894 cP of viscosity and 1.330 of refractive index; temperature: 25ºC. Other parameters specific to each technique were also defined. For size, a measurement angle of 173º backscatter and 3 measurements with 11 runs each were set. For the zeta potential, the dielectric constant of the dispersant was selected (78.5), the model used for the calculations, was the Smoluchowski model, and 3 measurements of 10 to 100 runs with 15 seconds of interval between them were performed. Zeta potential was measured after particle size, as it may damage the samples.

3.2.2 Nanoparticle Tracking Analysis (NTA)

Quantification of the NPs was performed by nanoparticle tracking analysis (NTA) in a NanoSight NS300 NTA Dev Build 3.2.16 equipped with an sCMOS camera. This technique is similar to DLS since it measures the scattered light of the samples, but it can also record the samples, resorting to a camera, through which we can analyse the NPs on an individual basis, and obtain the NPs concentration.

To prepare the samples for the analysis, sequential dilutions were performed with ultrapure water in order to obtain concentrations with a magnitude of around 10^8 NP/mL. Three videos of 30 seconds were recorded with the camera settings being: camera level 14, slider shutter 1259, slider gain 366, at 21 ºC, and with a syringe pump speed of 40. The data acquisition and processing were performed using the NanoSight NS300 NTA 3.0 software, using a detection threshold of 5. Analysis was performed by Ana Rita Pinto at i3S.

3.2.3 Fluorescamine Assay (AMP quantification)

Flourescamine is a non-fluorescent compound that reacts rapidly with primary amines to form highly fluorescent moieties, which allows the quantification of the AMP grafted to the NPs. First, a calibration curve was done to correlate AMP concentration with fluorescence intensity. For that, a solution with a known concentration of AMP was prepared, in this case 1024 µg/mL, and serial dilutions were performed in a black 96-well plate, to obtain a range of AMP concentrations from 512 to 0.125 µg/mL. Then, 50 µL of fluorescamine dissolved in acetone at 3 mg/mL were added to 150 µL of the NPs suspensions. Controls of fluorescamine (150 µL of water and 50 µL of the fluorescamine solution) and water (200 µL of ultrapure water) were also prepared. The plate was then transferred to the Synergy MX microplate reader to obtain the fluorescence of the samples using 400/460 nm excitation-emission wavelengths.

To quantify the AMP in the AMP-NP samples, fluorescence was measured through the same procedure. NPs samples were diluted in water by 1:4 to obtain fluorescence values within the range of the calibration curve.

3.2.4 Circular Dichroism (CD)

CD was used in an attempt to determine the secondary structure of the AMP when grafted to the NPs. The evaluation was performed through CD on a JASCO J-815 spectropolarimeter, equipped with a temperature-controlled cuvette and controlled by the Spectra manager software. Three samples were analysed, one containing only the AMP solution, the second containing bare NPs, and the third containing AMP grafted NPs. Samples were prepared by dilution in 10 mM sodium phosphate, pH 7.4, and 100 mM sodium fluoride, adjusting the AMP concentration of the free AMP and AMP-NPs to 30 µM, and using the same number of particles as the AMP-NPs for the bare NPs sample.

Before the measurements, all samples were incubated at 37 ºC for 30 min. Far-UV CD spectra were recorded between 195 and 260 nm using a 1 mm path length cuvette. CD spectra were acquired with a scanning speed of 100 nm/min, an integration time of 1 s and using a bandwidth of 1 nm. The spectra were averaged over 16 scans and corrected by subtraction of the buffer or buffer plus NPs signal. The results are obtained in molar ellipticity (θ), which is related to the absorbance (θ=32.98 ΔAbs), and are represented in a graph correlating ellipticity (θ) and wavelength (nm).

3.3 GUVs Production

The production of GUVs, followed a protocol previously optimized by the group [80].

First, the lipids 1,2-dioleoyl-*sn*-glycero-3-phosphatidylcholine (DOPC) and 1-palmitoyl-2-oleoyl-*sn*-glycero-3-phosphatidylglycerol (POPG) were weighed, in a 7:3 DOPC:POPG molar ratio, to mimic the composition of the membrane of gram-positive bacteria, and fluorescent 1,2-dipalmitoyl-*sn*-glycero-3-phosphoethanolamine-N-(7-nitro-2-1,3-benzoxadiazol-4-yl)

(DPPE-NBD) (Avanti Polar Lipids, Inc.; Alabama, USA) in a 0.2 molar percentage was added to allow direct observation by fluorescence microscopy. To formulate 1mL of a 10mM lipid stock solution the following quantities of lipids were weighted: 5.5 mg of DOPC, 2.31 mg of POPG, and 0.174 mg of DPPE-NBD, and then dissolved in chloroform:methanol (9:1) in a glass container covered from light. This solution could be stored up to three weeks for future productions, at -20ºC.

Having the lipidic solution prepared, the electroformation process was initiated, which was done by resorting to a Vesicle Prep Pro (Nanion Technologies, München, Germany). The equipment conditions were verified previous to the electroformation process, for that, a multimeter was used to identify and access the state of the conductive side of the two ITO-slides, they were considered in good conditions when the values were below 100 Ω. After placing one of the slides in the Vesicle Prep Pro chamber, with the conductive side facing upwards, 20 µL of the lipid solution was slowly added to the slide. Then the solvent was left to evaporate completely for a few minutes, resulting in a dry lipid film on the slide. An 18 mm diameter O-ring and grease (provided with the equipment), were used to help fix the ring around the dried lipidic film.

To produce GUVs mimicking the membranes of Gram-positive bacteria, 280 µL of a hydration solution of sucrose 280 mM was added to the interior of the O-ring. To produce GUVs mimicking the membranes of Gram-negative bacteria, the hydration solution of sucrose contained 0.033 mg of LPS from *P. aeruginosa* (Sigma-Aldrich; Missouri, USA) (corresponding to 17% m/m of the lipidic mass present in the 20 µL used to form the lipidic film). At this step, the chamber was closed by placing the second ITO-slide with the conductive side facing downwards.

Having followed the previous steps, it was then possible to turn on the Vesicle Prep Pro and start the electroformation process. The parameters used are in the table 3.2.

Table 3. 2 - Parameters chosen in the Vesicle Prep Pro for the electroformation process.

Temperature: 37 ºC	**Frequency**: 5 Hz
1- Temperature establishment 5 minutes	
2- Rise: applied voltage from 0 to 3V 5 minutes	
3- Electroformation: alternating voltage of 3V (+3 V and -3 V peaks) 120 minutes	
4- Fall: applied voltage from 3 to 0 V 5 minutes	

After the electroformation process, the chamber was disassembled, and the GUVs were carefully collected with a micropipette, performing up and down movements before transferring them into an eppendorf. Subsequently, 560 µL of sucrose 280 mM solution were added to the recovered GUVs solution to obtain an approximate dilution of 1:3 (adjusted to the volume of GUVs recovered).

Table 3. 3 - Chemical properties of the lipids used in GUVs production.

Identifier	Name	Molecular Weight (Da)
DOPC	1,2-dioleoyl-sn-glycero-3-phosphatidylcholine	786.113
POPG	1-palmitoyl-2-oleoyl-sn-glycero-3-phosphatidylglycerol	760.076
DPPE-NBD	1,2-dipalmitoyl-sn-glycero-3-phosphoethanolamine-N-(7-nitro-2-1,3-benzoxadiazol-4-yl)	872.090

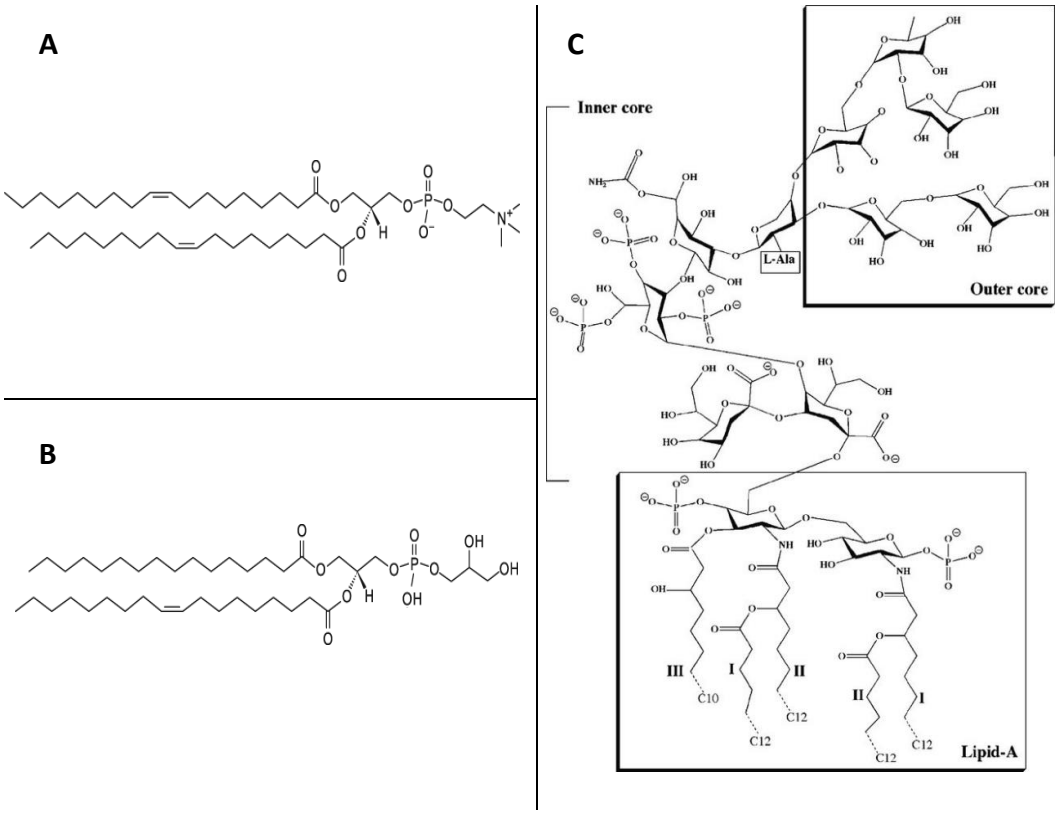

Figure 3. 3 – Chemical structure of (A) DOPC, (B) POPG, and (C) LPS from P. aeruginosa [20].

3.4 GUVs sedimentation

The produced GUVs are in suspension which makes microscopy observation very difficult due to their movement. To overcome this problem a sedimentation protocol was optimized.

First, to achieve GUV sedimentation, a sugar gradient was created by adding a glucose solution of 280 mM to the GUVs suspension in a 1:1 molar ratio. This step decreased the density

of the aqueous solution, maintaining the sucrose inside the GUVs, as sucrose and glucose have the same saccharide concentration, isotonic conditions were created. As sucrose has a higher density than glucose, larger GUVs sediment. Addition of glucose was tested at two different time points, after 5 and 20h after GUVs formation.

Another approach tested was an adhesive coating from Cell-Tak from Corning, which is used to produce coatings on substrates to immobilize cells or tissue. The coating was prepared according to manufacturer's instructions using the adsorption method. Initially, the amount of Corning Cell-Tak needed for the experiment was calculated according to the area of the wells. The density of Cell-Tak should be around 3.5 µg/ cm^2 of surface area, having considered this and the total volume needed, the Cell-Tak solution was diluted in a neutral buffer, Sodium Bicarbonate, and a volume of 1N NaOH, equal to half the volume of Cell-Tak, was added to obtain a range of pH from 6,6-8, which provides optimal coating performance.

Then 50 µL were dispensed into each well of a µ-Slide 18 Well IbiTreat and incubated for 20 minutes to let the adsorption occur. After the incubation time, each well was aspirated and washed with sterile water to remove the remaining Cell-Tak solution. Finally, the wells were ready to use, if they were not used right away, they were saturated with Argon and stored with desiccant.

3.5 GUVs Characterization

3.5.1 Inverted Fluorescence Microscope

Before proceeding with interaction studies, GUVs were first observed using an inverted fluorescence microscope, Axiovert 200M from Zeiss. First, the lamp (HBO Mercury short-arc lamp without reflector, 103 W/2) was turned on and allowed to stabilize for 10 minutes. Meanwhile, the obtained GUVs suspensions were diluted by a factor of 1:10 in glucose 140 mM, and 50 µL were transferred to a µ-Slide 18 Well IbiTreat (previously treated or not with Cell-Tak).

The slide was then placed on the stage and centred with the light path. The 100x objective was selected along with the filter unit, namely a green filter (395/509), to allow the observation of the NBD labelled GUVs.

The samples were then processed using ImageJ software, to evaluate size and sedimentation.

3.5.2 Fourier-transform infrared (FTIR) spectroscopy

Fourier-transform infrared (FTIR) spectroscopy was used to characterize the GUVs, specifically in an attempt to evaluate the incorporation of the LPS in the GUVs membranes. With this purpose, three samples were analysed, pure LPS, and GUVs with and without LPS, which mimicked Gram-negative and Gram-positive bacteria respectively.

All the samples were analysed in a Frontier 2000 FT-IR spectrometer (PerkinElmer, Massachusetts, USA) with a mid-infrared (MIR) triglycine sulfate (TGS) detector at the i3S Biointerfaces and Nanotechnology scientific platform. The LPS, which was in a solid-state, was compressed into a pellet and loaded into the equipment. For the GUVs samples as they were in solution, a drop of 2-3 µL was loaded into the equipment a few minutes before the analysis, to allow the water to evaporate and decrease its interference in the spectra.

The spectra were obtained using 32 scans, at a spectral resolution of 4 cm^{-1}, and wavenumber ranging from 4000 to 400 cm^{-1}.

3.6 Interaction studies between AMP/NPs/AMP-NPs and GUVs

3.6.1 Confocal Laser Scanning Microscopy

The interaction between free AMP, bare NPs and AMP-NPs, with the GUVs was analysed through confocal laser scanning microscopy on a Leica Stellaris 8 confocal microscope equipped with the Leica Application Suite X package. All the images were acquired with a resolution of 1024×1024 using a 63X/1.4 oil immersion objective. The NBD, present in the GUVs membranes, was excited at 460 nm and the emission was measured in the 480-540 nm range. The probe FKR560, present in the NPs, was excited at 562 nm and the emission was measured between 590 and 650 nm.

To prepare the samples for the observation, first, the GUVs solution was diluted in glucose 140 mM in a ratio of 1:10, which was then transferred to 35 mm imaging dishes with polymer coverslip bottom (µ-Dish 35 mm). This dilution decreased the number of GUVs in the sample which allowed a better observation of the interaction. The dish was then transferred to the microscope to access the good state of the GUVs, and to choose a region with an adequate number of GUVs with the desired size.

Having a region selected, free AMP, bare NPs or AMP-NPs were added to the GUVs preparation immediately before imaging, to obtain concentrations of 4, 8, 16, 32, and 64 µg/mL of AMP in the samples of free AMP and AMP-NPs, and for the bare NPs an equal number of NPs as in the AMP-NPs samples was used. After the addition images were recorded every 10 seconds for a total of 20 minutes. Finally, the images were processed using ImageJ software to evaluate the interaction.

3.7 Statistical Analysis

Statistical analysis was performed using GraphPad Prism version 9.0.2 for Mac OS X (GraphPad Software, California, USA). Unpaired t-test with Welch's correction was used to compare AMP-NPs with the respective control. Values are presented as mean ± standard deviation (SD). Statistical significance is indicated as ****$p \leq 0.0001$.

Chapter 4 – Results and Discussion

4.1 AMP-NP characterization

4.1.1 Dynamic and Electrophoretic Light Scattering

The size distribution and surface charge of AMP-NPs and respective control of bare NPs were determined.

Bare NPs have a size of approximately 100 nm, while AMP-NPs have around 140 nm, presenting a slight increase in size after AMP grafting. Both samples present a PdI lower than 0.3 (0.1 for the bare NPs and 0.2 for the AMP-NPs) demonstrating that the population is essentially homogeneous in both. The slight increase in size may indicate successful AMP grafting.

Regarding the surface charge, or Zeta Potential (ZP), bare NPs have a negative ZP (-2.9 mV ± 0.9) due to the presence of carboxylic groups in PLGA. AMP-NPs present positive ZP values, more specifically 12.2 ± 1.1 mV, demonstrating successful AMP grafting. AMPs are cationic therefore their addition causes a shift to positive ZP values.

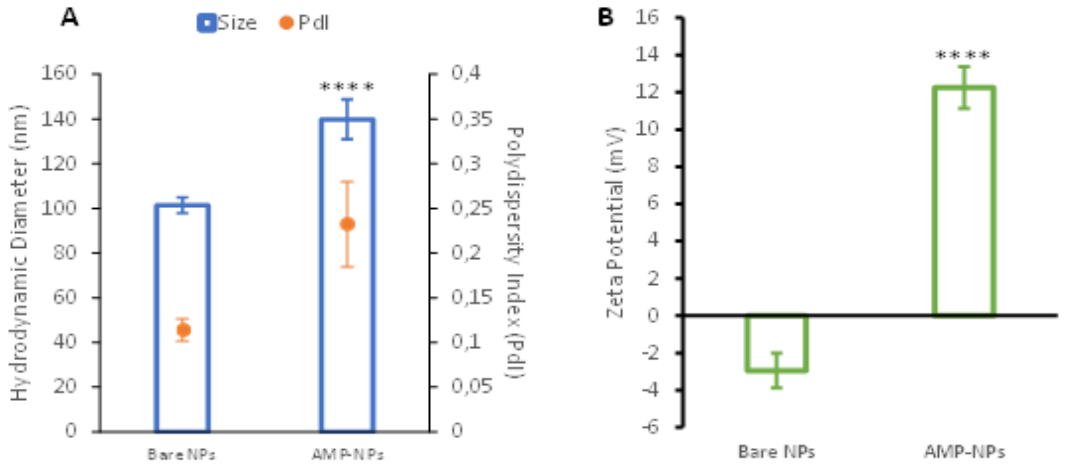

*Figure 4. 1 - (A) Hydrodynamic diameter, PdI and (B) ZP of fluorescent bare NPs and AMP-NPs. Values are presented as mean ± SD (n=3). Unpaired t-test with Welch's correction was used to compare AMP-NPs with the respective control. Values are presented as mean ± standard deviation (SD). Statistical significance is indicated as ****p ≤ 0.0001.*

The results regarding size and zeta potential, obtained for the NPs produced in this work with fluorescently labelled PLGA-PEG are similar to the ones previously obtained by the group using non-labelled PLGA-PEG (manuscript under revision) meaning that the addition of a fluorescence probe does not affect the size and zeta potential of AMP-NPs.

4.1.2 Nanoparticle Tracking Analysis

The NTA allowed the quantification of the number of particles present in both bare NPs and AMP-NPs suspensions. The results obtained are in the table 4.1, as it is possible to observe both samples have an approximate number of particles, so there are no significant differences in the NPs concentration before and after grafting the AMP.

Figure 4.2 are representative images captured during the NTA, it is possible to identify individual particles with similar sizes for both bare NPs and AMP-NPs, observations that go accordingly to the results obtained by dynamic light scattering.

Table 4. 1 - Concentrations of bare NPs and AMP-NPs obtained through NP tracking analysis.

	Concentration (particles/mL)
Bare NPs	$1.17 \times 10^{14} \pm 9 \times 10^{12}$
AMP-NPs	$2.12 \times 10^{14} \pm 2 \times 10^{13}$

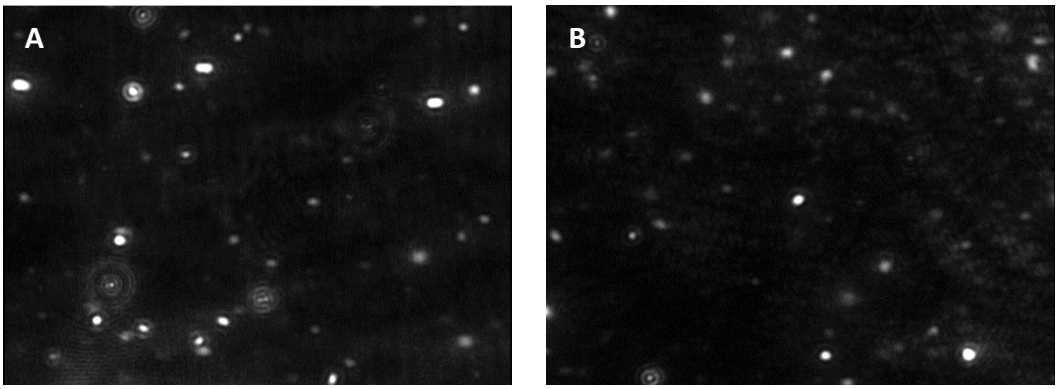

Figure 4. 2 - Representative images of (A) bare NPs and (B) AMP-NPs captured during the nanoparticle tracking analysis.

4.1.3 Fluorescamine Assay

The fluorescamine assay was used to quantify the amount of AMP grafted. The average AMP concentration obtained from 3 independent samples was 323 ± 32 µg/mL, which also goes accordingly to the previous results obtained by the group for non-labelled AMP-NPs (manuscript under revision).

The quantifications of AMP concentration and number of particles are crucial for the interaction studies as the AMP quantification allows to study the interaction with the membranes with specific concentrations of AMP, and the NPs quantification, enables to adjust the concentration of the control bare NPs to the same number of particles present in the AMP-NP samples.

4.1.4 Circular Dichroism (CD)

Litlle is known about the secondary structure of AMPs upon conjugation with NPs, CD was performed with three different samples, free AMP, bare NPS and AMP-NPs, in an attempt to study the influence of the conjugation in the secondary structure of the AMP. AMP concentration was adjusted to 30 mM in the free AMP and AMP-NPs samples, and the bare NPs were adjusted to the same number of NPs present in AMP-NPs sample. All samples were tested in aqueous buffer. The obtained spectra are in the figure 4.3.

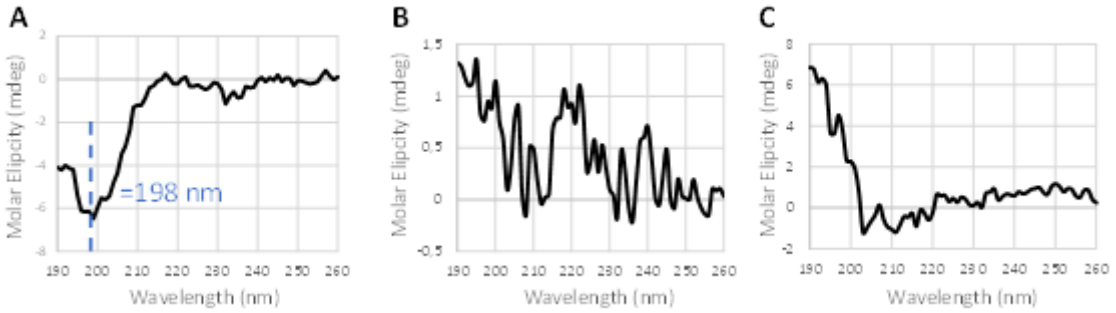

Figure 4. 3 - CD spectra of (A) AMP, (B) bare NPs and (C) AMP-NPs.

The CD spectra of the MSI-78(4-20) in aqueous buffer (A) presented a negative minimum at 198 nm indicating that the peptide presented a random coil conformation. These results are in agreement with studies published by our group, which performed CD for the AMP in aqueous solutions without and with the presence of LUVs mimicking eukaryotic and bacterial cell membranes. They concluded that the AMP had a random coil conformation in aqueous buffer and in the presence of eukaryotic LUVs, suggesting that there is no toxicity towards eukaryotic cells, and acquired an *α*-helical conformation when in the presence of LUVs mimicking the bacterial membrane, indicating an interaction with bacterial cells [47].

Analysing the spectra of the bare NPs (B) a great absorption in the zones of interest for the determination of the peptides' secondary structure was observed. Regarding the result from the AMP-NPs (C), no characteristic peaks for random coil or secondary structures were detected, meaning that the spectrum is inconclusive. This is a result of the high absorption of bare NPs.

The study of the secondary structure of immobilized AMPs with CD is not simple, mainly because there is always interference of the surface where the peptides are immobilized. However, some studies have combined CD with other advanced techniques like, all-atom molecular dynamics simulation and sum frequency generation vibrational spectroscopy, and were able to determine the AMPs secondary structure [79 - 80].

4.2 GUVs Sedimentation Optimization and characterization

4.2.1 Fluorescence Microscopy

4.2.1.1 GUVs mimicking Gram-Positive bacterial membranes

After production, GUVs mimicking Gram-positive bacterial membranes were observed in the inverted fluorescence microscope. GUVs recovered in sucrose (figure 4.4) presented a lot of movement which made observation and characterization very difficult.

To overcome this problem, two strategies were tested, one resorted to the creation of a density gradient to sediment the GUVs using glucose, and the other to deposit an adhesive coating on the observation wells/dishes to immobilize the GUVs on the surface bottom [81- 82].

The figure 4.4 shows representative images of GUVs upon addition of glucose 5 and 20 hours after production. In both conditions, GUVs presented much less movement than when recovered in sucrose only, as it is possible to observe well defined GUVs in these images. When comparing the two time points, performing the sedimentation step 20 hours after the GUVs production, lead to the observation of more GUVs, with larger diameters from 8 µm to 18 µm, with an average of around 12 µm. While performing the sedimentation step 5 hours after its production lead to GUVs with smaller sizes, with diameters ranging from 2.5 µm to 7 µm, with an average size of 5 µm, more similar to the size of bacteria, which is around 2-3 µm.

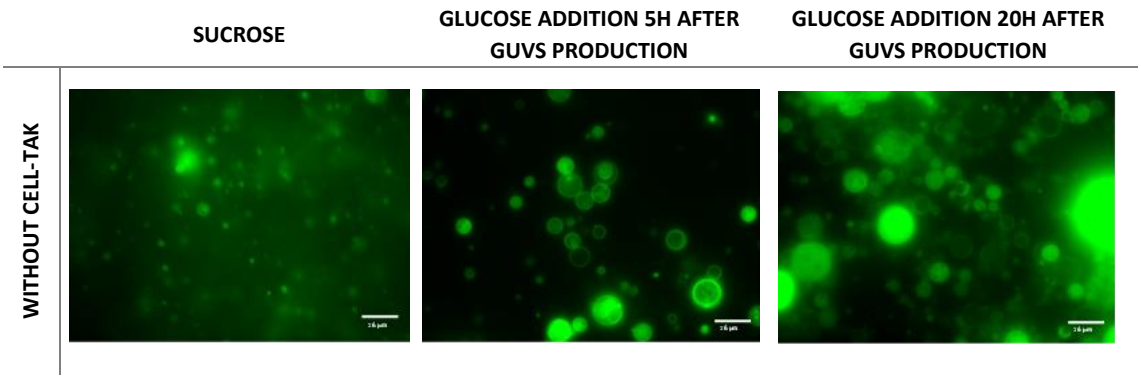

Figure 4. 4 - Inverted fluorescence microscope images of GUVs recovered in sucrose, and with the addition of glucose 5 and 20 hours after production. Images were taken with the 100x oil objective.

To test the second strategy, the *Cell-Tak* adhesive coating was prepared and GUVs observed under the previous optimized conditions, meaning that the sedimentation step was performed with glucose after 5h (figure 4.5). The observation demonstrated that in fact some GUVs were immobilized in the bottom of the well, however, GUVs presented smaller sizes and some deformation of the membranes. Moreover, the images presented some unidentified shapes that could be from the coating or eventually from degraded GUVs.

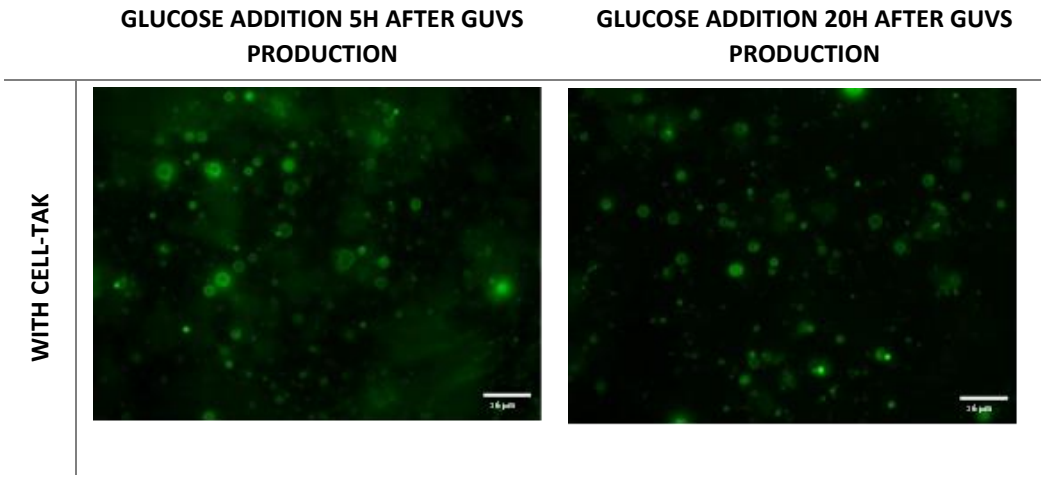

Figure 4. 5 - Inverted fluorescence microscope images of GUVs with the addition of glucose 5 and 20 hours after production on wells previously coated with Cell-Tak. Images were taken with the 100x oil objective.

Considering these results, from this point forward GUVs were observed after sedimentation upon addition of glucose after 5h post-production and without using the Cell-Tak coating.

4.2.1.2 GUVs mimicking Gram-Negative bacterial membranes

For the production of GUVs mimicking the membranes of Gram-Negative bacteria, LPS from *P. aeruginosa* was added at the step of hydration dissolved in the sucrose solution, to obtain 17% m/m of the lipidic mass. This method was based on previous studies performed by Montis et al [79].

GUVs were recovered in sucrose only or glucose was added 5 hours after production. Representative images in figure 4.6.

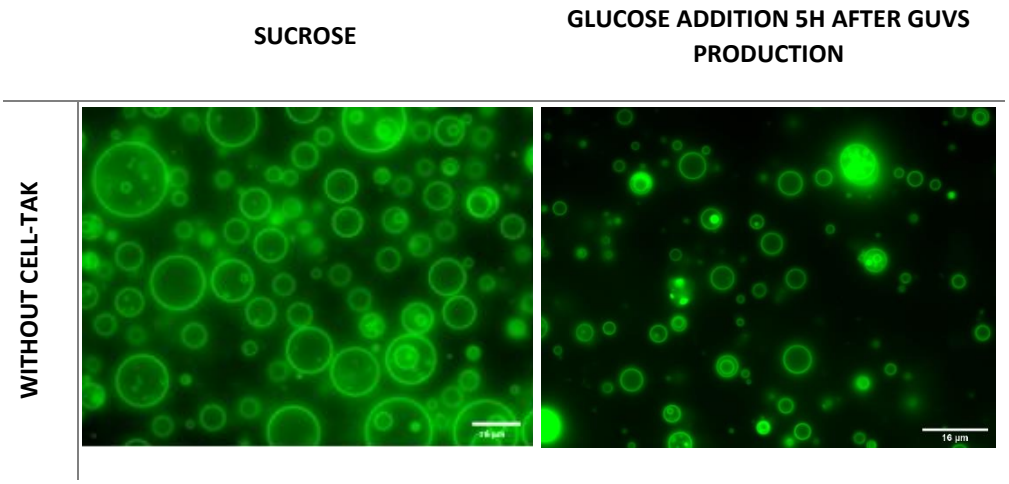

Figure 4. 6 - Inverted fluorescence microscope images of GUVs mimicking Gram-Negative bacteria recovered in sucrose only or with the addition of glucose 5 hours after production. Images were taken with the 100x objective.

In this case, it was possible to see well defined GUVs even without the sedimentation process, as they did not present a lot of movement when recovered in only sucrose also. The

GUVs recovered in sucrose only, presented sizes from 4 µm to 13.5 µm, with the average size being around 9.5 µm. The GUVs that were that were subject to the sedimentation process presented a slight reduction in size, with GUVs varying between 3 µm and 10 µm, with an average of 6 µm.

As the GUVs that undergo through the sedimentation process presented sizes more similar to the bacteria, and to maintain the conditions of the experiment for both types of GUVs, the sedimentation process 5 hours after production was used.

4.2.2 Fourier-transform infrared (FTIR) spectroscopy

Even though GUVs with LPS, to resemble the membrane of Gram-Negative bacteria have been reported a number of times in the literature [77], confirmation of LPS insertion is not performed, so in an attempt to address this issue, FTIR was performed on pure LPS and on GUVs with and without LPS. FTIR spectra are shown in figure 4.7.

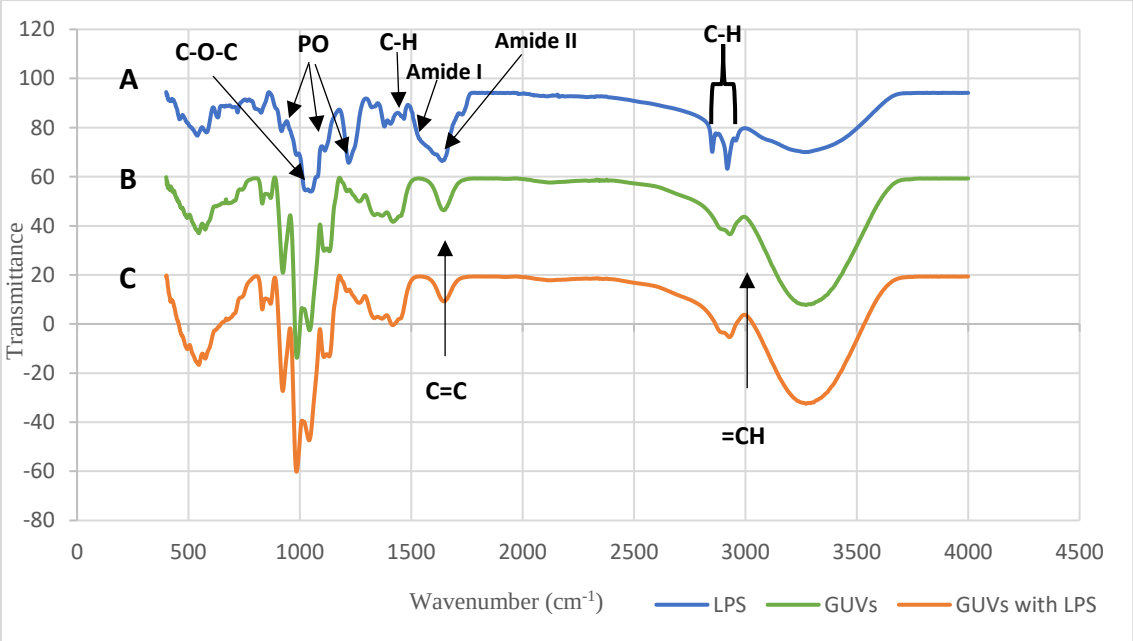

Figure 4. 7 – FTIR spectra of (A) LPS, (B) GUVs mimicking Gram-positive bacteria (without LPS) and (C) GUVs mimicking Gram-negative bacteria (with LPS).

In the LPS spectrum (A) it is possible to observe characteristic stretching vibrations of lipid A, namely of C-H (2820-2940 cm^{-1}; 1460-1470 cm^{-1}) and phosphate (PO) (1200-1265 cm^{-1}, 1106 cm^{-1}, and 960-983 cm^{-1}), and the C-O-C stretching of polysaccharides at 1050-1085 cm^{-1} characteristic of the O-antigen [85]. Additionally, at around 1650 and 1550 cm^{-1}, the vibrations can be attributed to the amide I and II modes of the LPS molecule [86].

In the spectrum of (B) GUVs without LPS it is also possible to identify some the characteristic vibrational peaks of C-H bending (833-903 cm^{-1}), C=C bending (944-967 cm^{-1}) C-O stretching (1086-1133 cm^{-1}), C=C stretching at 1653 cm^{-1} and C-H asymmetric stretching (2933-2929 cm^{-1}).

When analysing the spectra of (C) GUVs that mimic Gram-Negative bacteria, with LPS and (B) GUVs that mimic Gram-Positive bacteria, without LPS, there are no significant differences between them. A possible explanation for this besides the similar spectra due to structural similarities between lipids, is the reduced amount of LPS in the composition of the GUVs comparing to DOPC and POPG.

4.3 Interaction with GUVs

The interaction of free AMP, bare NPs, and AMP-NPs with GUVs mimicking gram-positive and gram-negative bacteria was observed using confocal microscopy. The AMP and AMP-NP samples were tested in five different concentrations from 4 to 64 μg/ mL of AMP, bare NPs matched the number of particles used for the AMP-NPs samples. The interaction was recorded in time-lapse, and representative images of the interaction after 10 and 20 minutes are shown in the tables 4.8 to 4.11. All the images present the merge of the green and red channels, being the GUVs labelled in green and the NPs labelled in red, except for the images with free AMP (not labelled) which exhibit only green fluorescence from the GUVs.

Regarding the interaction of the AMP with GUVs mimicking the Gram-Positive bacterial membrane, after 10 minutes of the addition it is already possible to observe the interaction between the AMP and the GUVs, demonstrated by GUVs deformation and agglomeration. This interaction is only observed at the concentration of 16 μg/ mL and higher, which indicates a correlation between the concentration and the interaction. In higher concentrations there are fewer GUVs and the ones present, are agglomerated and with irregular shapes as a result of stronger interactions. In the images with 20 minutes of interaction, the lower concentrations also show signs of interaction, as they present deformed and agglomerated GUVs, and the effect of concentration is still present, as higher concentrations present fewer GUVs. These results, are in agreement with the antimicrobial activity of the AMP against Gram-positive bacteria, namely *S. aureus* which was reported to be 16-32 μg/ mL (manuscript under revision).

Regarding the images obtained for the interaction between bare NPs and GUVs mimicking the Gram-Positive bacterial membrane, it is very clear that they are present in the solution, as it is possible to observe red structures, as they start to aggregate in higher concentrations. However, no interaction seems to occur with GUVs, as GUVs do not suffer alterations even after 20 minutes and in the presence of the higher NPs concentrations. Moreover, GUVs remain with their original circular shape, with no overlay of the green and red channels. This observation proves that there is no interaction between the GUVs and bare NPs. Although bare NPs do not aggregate in water as shown by DLS analysis, aggregation seems to be induced in the sucrose/glucose solution used to recover and sediment the GUVs.

In the results obtained for the interaction between AMP-NPs and GUVs mimicking the Gram-Positive bacterial membrane, there are clear signs of interaction for all the concentrations tested, even only after 10 minutes of interaction, as it is possible to observe an overlay of both green and red channels in the membranes of the GUVs, which present a yellow colour. At higher concentrations fewer GUVs are observed due to the disruption of their membranes. The phenomenon of GUVs disruption is visible under time-lapse. Moreover, some aggregation of the NPs is observed for the concentration of 64 μg/ mL. After 20 minutes, the

interaction continues as evidenced by the decrease in the number of GUVs for all concentrations. The correlation between concentration and effect is still verified as higher concentrations show less GUVs due to their membrane disruption.

Although, both AMP and AMP-NPs interact with GUVs mimicking Gram-positive bacteria, there are some differences between them. First, they seem to differ in their mechanism of action, the AMP starts to change the GUVs to irregular shapes and induces GUVs aggregation before eventually disrupt the GUVs membrane, while the AMP-NPs seem to disrupt the membrane completely without inducing irregular shapes and aggregation. Second, when comparing the images after 10 minutes, the interaction appears to happen at lower concentrations for AMP-NPs as it is already present for the lower concentrations of 4 and 8 μg/mL, contrary to the AMP. Although MIC values reported by us for AMP and AMP-NPs do not differ in growth media (manuscript under revision), AMP-NPs were able to kill bacteria faster than the AMP alone, which correlates with the faster interaction of AMP-NPs for lower AMP concentrations.

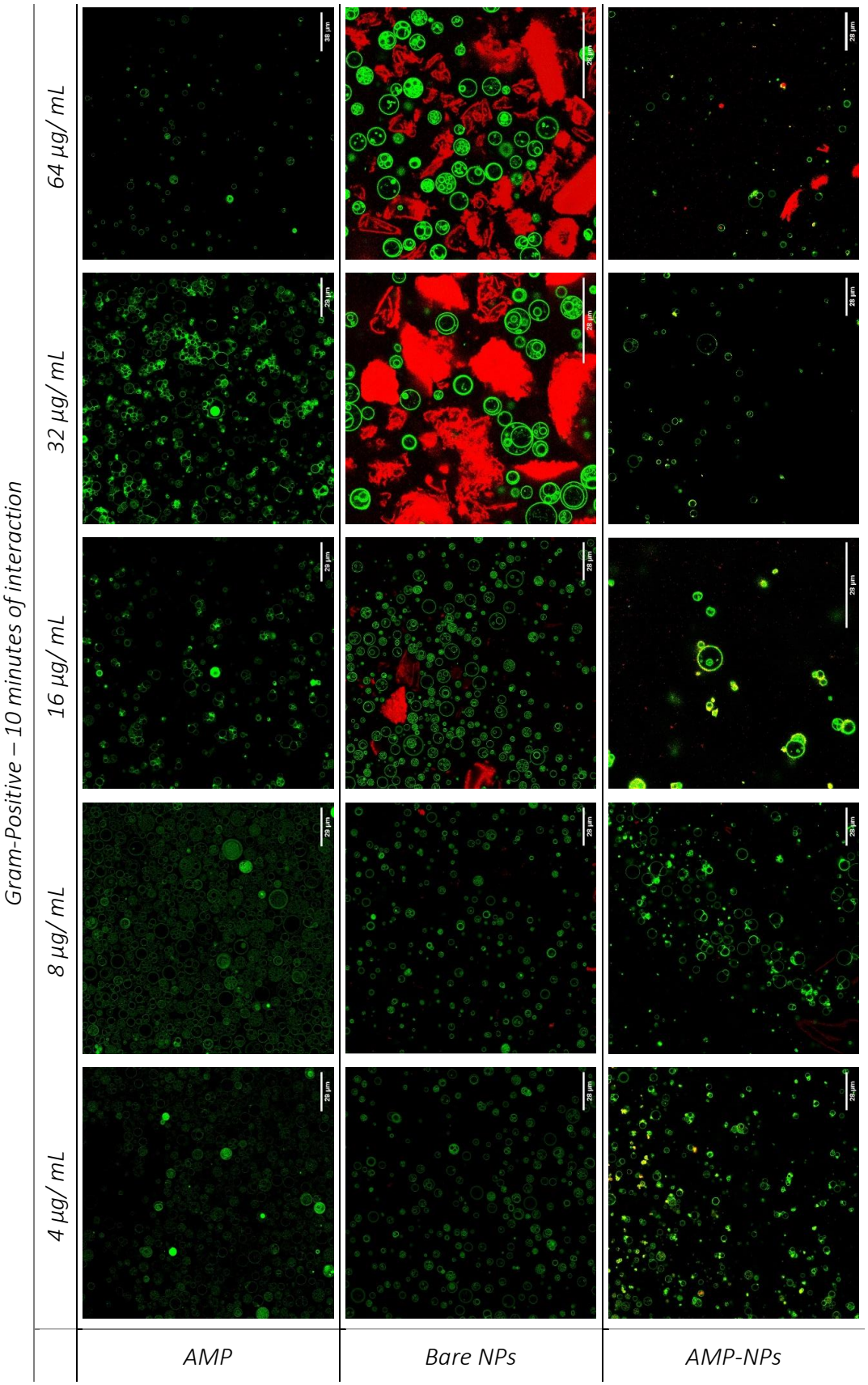

Figure 4. 8 - Images of GUVs mimicking the Gram-positive bacterial membrane upon interaction with AMP, bare NPs and AMP-NPs for 10 minutes. Images were captured in the confocal microscope with the 63X/1.4 oil immersion objective. GUVs are labelled in green and NPs labelled in red.

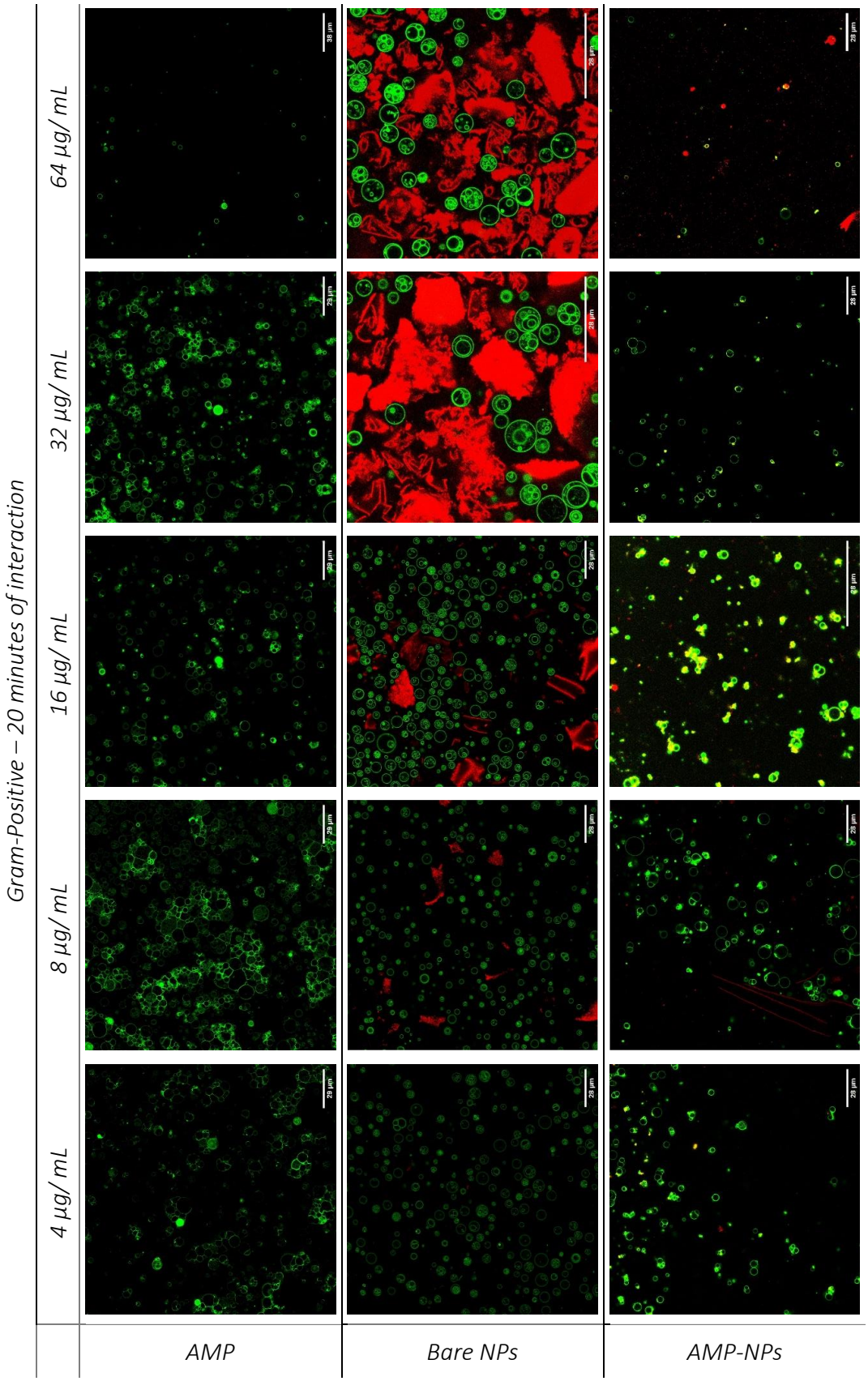

Figure 4. 9 - Images of GUVs mimicking the Gram-positive bacterial membrane upon interaction with AMP, bare NPs and AMP-NPs for 20 minutes. Images were captured in the confocal microscope with the 63X/1.4 oil immersion objective. GUVs are labelled in green and NPs labelled in red.

The interaction of AMP, bare NPs and AMP-NPs with GUVs mimicking the Gram-Negative bacterial membrane was also analysed. Regarding the AMP, 10 minutes after its addition some interaction with the GUVs is already observed, but only at the higher concentrations of 32 and 64 μg/ mL, as it is possible to observe GUVs aggregation and deformation only ate these concentrations. This indicates a correlation between the AMP concentration and the interaction. Analysing the images 20 minutes after its addition, it is also possible to observe the agglomeration and deformation of the GUVs at the 16 μg/ mL concentration, even though in a smaller extent when compared with the higher concentrations which already present less GUVs due to their membrane disruption. The MIC of the AMP against the Gram-negative *Pseudomonas aeruginosa* was reported to be 1-2 μg/ mL, however MIC results are obtained after an overnight incubation with the bacteria.

The results obtained for the bare NPs, are very similar to the ones obtained for the GUVs mimicking the Gram-Positive bacteria, meaning that no interaction between the bare NPs and GUVs occurs. GUVs do not suffer any alterations at any concentration, maintaining their original circular shape. A similar NP aggregation behaviour is observed for higher NP concentration at either 10 and 20 min of interaction.

Finally, the AMP-NPs show signs of interaction for all concentrations even after only 10 minutes of their addition, as its possible to observe the overlap of the green and red channels. Moreover, at concentrations of 16 μg/ mL and higher agglomeration and disruption of GUVs is observed, demonstrating once more the correlation between AMP-NPs concentration and interaction. Observing the images taken 20 minutes after the addition, the lower concentrations also show the agglomeration of the GUVs and their deformation, however the correlation between AMP-NPs concentration and interaction is still evidenced with these processes occurring at a faster rate in the higher concentrations.

Comparing the interaction between the AMP and AMP-NPs, the latest seems to occur at lower concentrations and to be faster. Although AMP-NPs lose some activity in antimicrobial assays against Gram-negative bacteria when comparing to the AMP alone, killing kinetics is improved for bactericidal concentrations, which is in agreement with the results obtained with the GUVs [87].

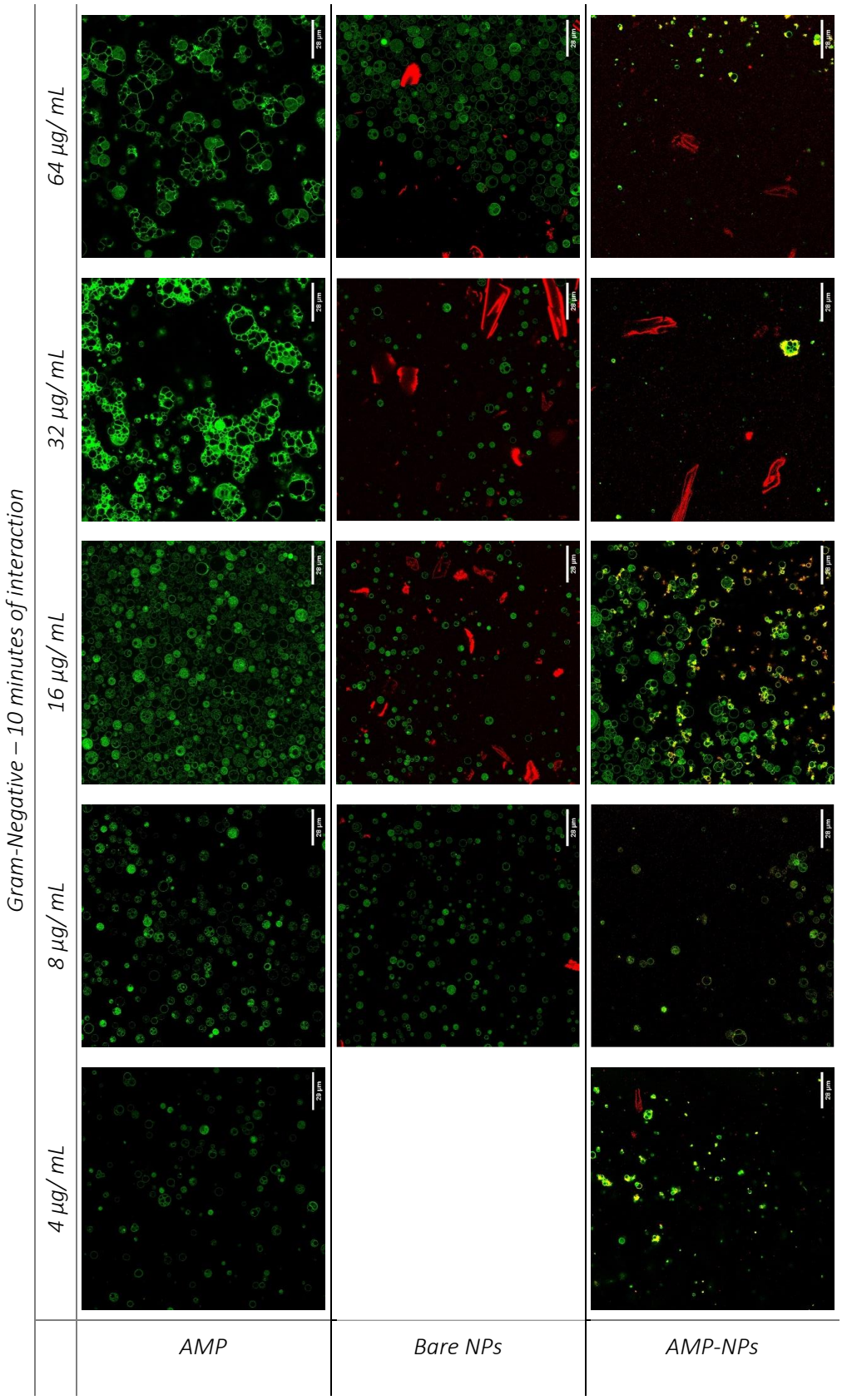

Figure 4. 10 - Images of GUVs mimicking the Gram-negative bacterial membrane upon interaction with AMP, bare NPs and AMP-NPs for 10 minutes. Images were captured in the confocal microscope with the 63X/1.4 oil immersion objective. GUVs are labelled in green and NPs labelled in red.

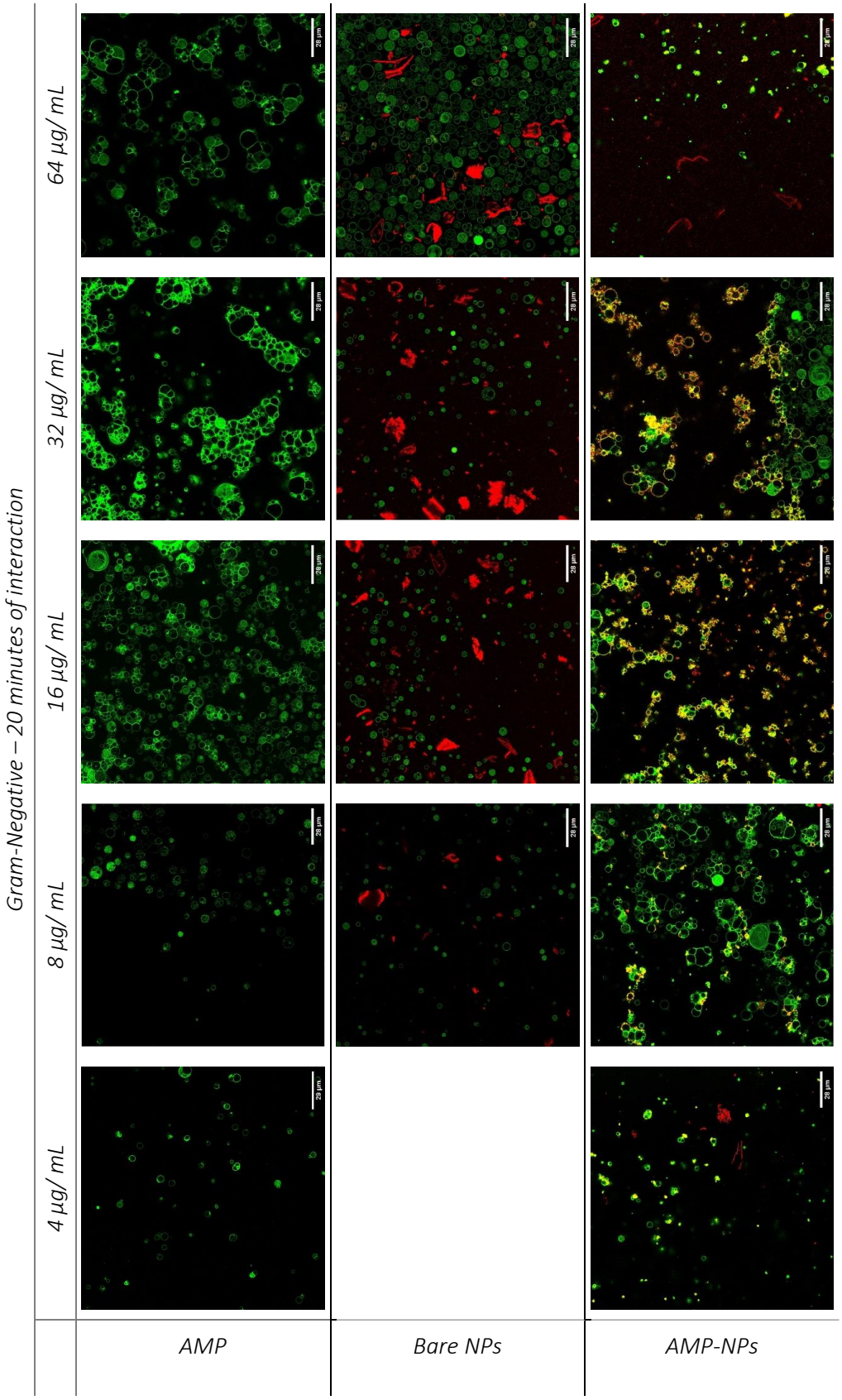

Figure 4. 11 - Images of GUVs mimicking the Gram-negative bacterial membrane upon interaction with AMP, bare NPs and AMP-NPs for 20 minutes. Images were captured in the confocal microscope with the 63X/1.4 oil immersion objective. GUVs are labelled in green and NPs labelled in red.

Comparing the results from the Gram-Positive with the Gram-Negative GUVs, it is possible to spot a great difference in the interaction with the AMP-NPs. While for the Gram-Positive GUVs, they seem to cause the complete disruption of the membranes, which makes them disappear without previous deformation and aggregation, for the Gram-Negative GUVs, AMP-NPs have an effect more similar to the AMP, where the GUVs start to aggregate and acquire an irregular shape.

It also seems that the interaction is slower with the Gram-Negative GUVs than with the Gram-Positive for both AMP and AMP-NPs. When comparing the concentrations of AMP of 4 and 8 μg/ mL after 20 minutes between the two types of GUVs, it is clear that there are a lot more regular GUVs in the Gram-Negative images. The same happens when comparing the results of the AMP-NPs, as the images from the Gram-Positive GUVs show significantly fewer GUVs.

However, the velocities of interactions cannot be precisely compared in this study, because this parameter can be influenced by several parameters that were not possible to control, such as the zone being observed, the distance to where the samples were introduced, and also the density of the GUVs in certain areas can delay the ability of the AMP and AMP-NPs to reach a certain area.

In the figure 4.12 zoomed images of AMP-NPs (16 μg/ mL of AMP) interacting with GUVs mimicking Gram-Positive and Gram-Negative bacteria after 15 min of interaction are presented. To better understand the exact location of the AMP-NPs, the fluorescence intensity of each channel was measured using ImageJ.

Analysing the intensity profile for the interaction of AMP-NPs with the Gram-Positive mimicking GUVs, the presence of two overlapping peaks in both colour channels is evident. This observation proves the colocalization of AMP-NPs and the GUVs membrane, meaning that there is an accumulation of cationic AMP-NPs at the surface of the anionic GUVs, most likely promoted by electrostatic interactions. It is also possible to observe some peaks of both channels inside of the GUVs, which may indicate AMP-NPs internalization and membrane degradation.

Analysing the interaction of AMP-NPs with the Gram-Negative mimicking GUVs, the results are similar. There is a clear overlap of both channels in the membranes of the GUVs, which is also represented in the fluorescence intensity profile graph by two peaks. This also confirms the accumulation of AMP-NPs at the membrane of the Gram-negative mimicking GUVs, promoted by electrostatic interactions due to the presence of negatively charged PG and LPS. However, when comparing the two graphs, in the second peak of graph B, the intensity of the red channel is higher than the green one, which may be explained by the different interaction that AMP-NPs have with GUVs containing LPS, which seems to cause AMP-NPs agglomeration, leading to a higher accumulation on the membranes. This phenomenon is also observed directly in the images, as yellow spots can be identified along the membrane.

Through these results, it is possible to conclude that the AMP-NPs interact with the GUVs membranes through electrostatic interactions, which leads to an accumulation of AMP-NPs on the membranes, and consequently their destabilization or disruption. These results go

according to previous studies about the mechanism of action of free AMP, meaning that their immobilization in the NPs did not significantly modify their mechanism of action [47].

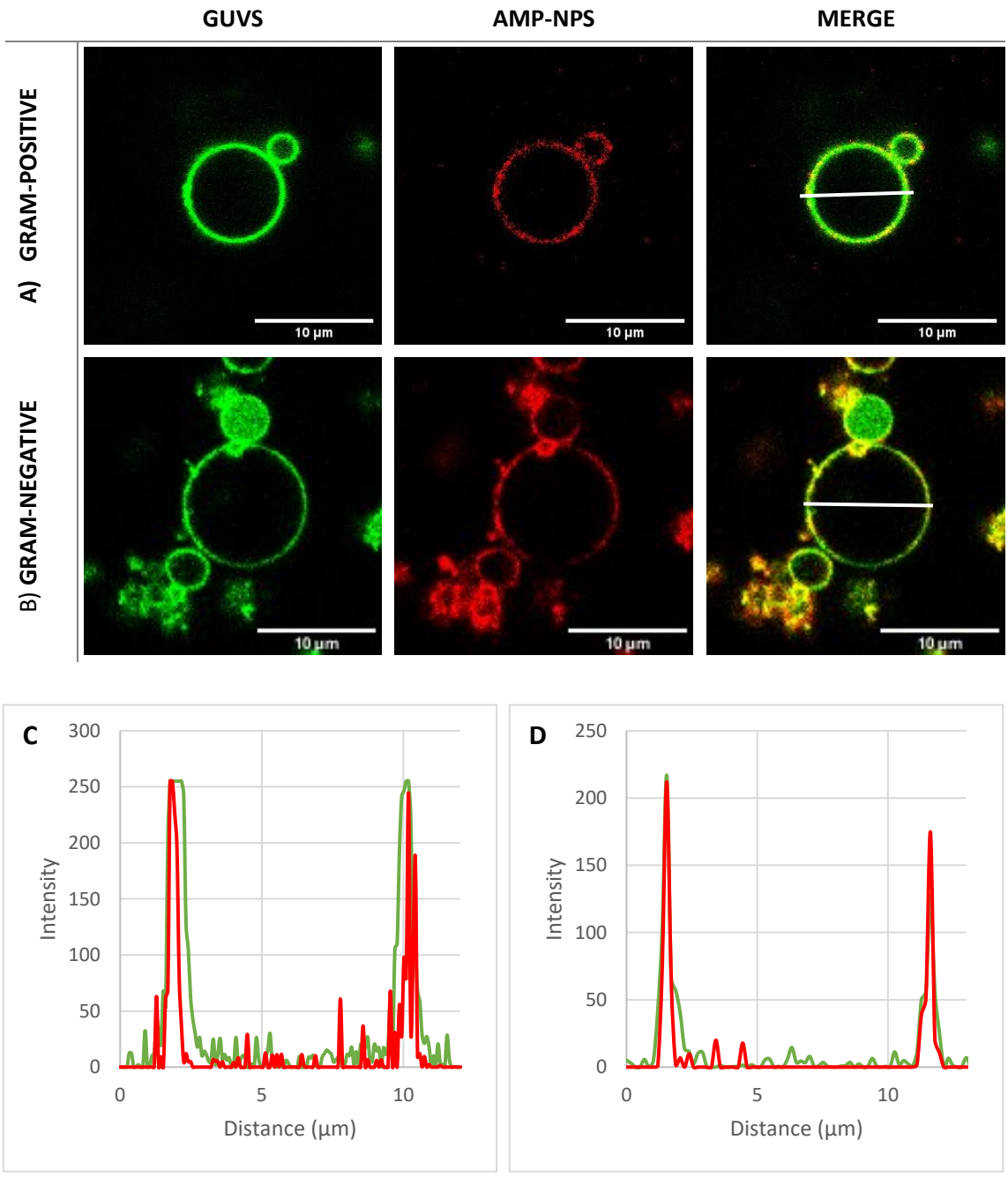

Figure 4. 12 – Confocal images of AMP-NPs interacting with GUVs reassembling the membranes of (A) Gram-Positive and (B) Gram-Negative bacteria, after 15minutes of interaction. NBD labelled GUVs in the green channel, FKR560 labelled AMP-NPs in the red channel, and the merge of both channels. Fluorescence intensity profiles of AMP-NPs interacting with (C) Gram-Positive and (D) Gram-Negative GUVs, with NBD (green line) and FKR560 (red line) intensities.

PLGA NPs interaction with GUVs mimicking eukaryotic membranes has been studied and very few interactions have been reported with this model membrane [84]. Regarding PLGA-PEG NPs, to our knowledge, no studies have been done regarding interaction with GUVs either mimicking eukaryotic or bacterial membranes. PEG is a non-fouling inert polymer therefore no

interactions are expected for bare NPs, being the cationic AMP surface functionalization expected to dictate the fate of the interactions.

Although most of the results here presented are in accordance with the antimicrobial activity studies of this conjugate against *S. aureus* and *P. aeruginosa*, it should be noted that the work was performed with simplistic membrane models that do not reproduce the complex and dynamic structure of an actual bacterial membrane. In this study, we can analyse in more detail the influence that LPS has in the interaction of the AMP and AMP-NPs with the membrane of Gram-Negative bacteria. The presence of LPS seems to promote a mechanism of action for AMP-NPs more similar the AMP alone, as the interaction behaviour of the AMP with both types of GUVs was similar to the interaction of AMP-NPs with GUVs containing LPS. In the presence of LPS deformation and agglomerates occurred, while sudden disruption, without deformation and aggregation, was observed for AMP-NPs with GUVs without LPS.

However, there are many other components that can have an influence. For instance, negatively charged TAs, present in the cell wall of Gram-positive bacteria may lead to alterations in the interactions. Nevertheless, interpretation and design of these models must consider the structure of Gram-positive and Gram-negative membranes, namely the fact that LPS is present in the outer membrane of Gram-negative bacteria and TAs are present in the peptidoglycan of Gram-positive bacteria.

Chapter 5 - Conclusions and Future Directions

AMPs are one of the most promising alternatives to combat infections caused by antibiotic resistant bacteria, and several improvement strategies have been investigated to overcome the challenges faced to reach clinical application, namely its conjugation with nanoparticles. Having AMPs so much potential, it is of extreme importance to understand their structure and mechanism of action, to consequently improve their efficacy in clinical use. Although this has been studied for free AMPs, there is not much literature about the structure and mechanism of action for AMPs conjugated to nanoparticles. In this context, the main objective of this work is to unravel the mechanism of action of AMPs when immobilized on NPs, in this specific case when the AMP MSI-78(4-20) is conjugated to PLGA-PEG NPs.

For that, first fluorescent PLGA-PEG NPs were produced by nanoprecipitation of a mixture of PLGA-PEG, PLGA-PEG-Mal and PLGA-PEG-FKR560 copolymers and then a cysteine-modified MSI-78(4-20) was grafted through a thiol maleimide reaction. To study the mechanism of action of the conjugate, fluorescently labelled GUVs were produced by electroformation, with a lipid mixture of DOPC, POPG and DPPE-NBD to mimic the membranes of Gram-Positive bacteria, and LPS was added to the composition to mimic the membrane of Gram-Negative bacteria. The interaction was analysed under confocal laser scanning microscopy.

Fluorescent NPs had a diameter around 140 nm, low polydispersity and a surface charge of 12.2 mV, both size and surface charge had an increase when compared to bare NPS, which indicates AMP immobilization. These results were similar to the ones obtained by the group for non-labelled NPs, meaning that the addition of fluorescence did not interfere with these parameters. CD was performed to access the secondary structure of the AMP after immobilization, however the results were inconclusive due to interferences of the NPs in the measurement.

Fluorescent GUVs mimicking Gram-Positive and Gram-Negative membranes were observed under an inverted fluorescence microscope to confirm its correct formation. Since the GUVs recovered in sucrose were in suspension and presented a lot of movement, a sedimentation step was added. Resorting to observations from the inverted fluorescence microscope we optimized this process, to the addition of glucose after 5 hours of GUVs production. To confirm the incorporation of LPS in the GUVs membranes mimicking Gram-negative bacteria, FTIR was performed to pure LPS and GUVs with and without LPS. The results

obtained did not allow us to draw conclusions, probably due to the low relative quantity of LPS present in the GUVs.

Finally, in the confocal microscope were recorded time-lapse videos of free AMP, bare NPs and AMP-NPs interacting with GUVs mimicking the membranes of Gram-Positive and Gram-Negative bacteria at five different concentrations. The AMP and AMP-NP samples were tested from 4 to 64 μg/ mL of AMP, and bare NPs matched the number of particles used for the AMP-NPs samples.

From the captured videos it was possible to conclude that the bare NPs did not interact with the GUVs with or without LPS, once they maintained their original shape throughout the whole time in solution, although they seem to aggregate in sucrose/glucose solutions at high concentrations.

Both AMP and AMP-NPs exhibit signs of interaction with GUVs mimicking Gram-Positive bacteria but in different ways. While the AMP-NPs seem to lead to the complete disruption of the membranes without causing previous deformation or agglomeration, the AMP starts to change the GUVs to irregular shapes and induces GUVs aggregation before eventual disruption. In these interactions it is also noticeable that the AMP-NP acts faster and at lower concentrations than the AMP.

Regarding GUVs mimicking Gram-Negative bacteria both AMP and AMP-NPs present interaction but in this case both lead to GUVs deformation and agglomeration before disrupting their membranes. Similarly, to the GUVs mimicking Gram-Positive bacteria, AMP-NPs seem to interact at lower concentrations and faster than then AMP.

When comparing the interaction between the GUVs mimicking the Gram-Positive and Gram-Negative bacteria it seems that, for both AMP and AMP-NPs, the interaction is slower with the Gram-Negative GUVs. Also, the interactions with both types of GUVs, are in agreement with previous studies which showed an improved killing kinetics of the AMP when immobilized in the NPs.

Finally, the fluorescence intensity of each channel in two representative images of AMP-NPs interacting with GUVs mimicking the Gram-Positive and Gram-Negative bacteria, was analysed to assess the exact location of the AMP-NPs. We concluded that the AMP-NPs colocalize with the GUVs membranes, meaning that they accumulate on the membranes most probably due to the establishment of electrostatic interactions. These results go according to previous studies about the mechanism of action of free AMP.

It is also possible to conclude that the absence of LPS in the membranes leads to a different interaction for AMP-NPs causing the burst of the membranes. This may point out to a different mechanism of action of AMP-NPs towards Gram-positive and Gram-negative bacteria.

As future work, the complexity of the models may be increased, for instance by adding other components to the GUVs composition, for example TAs in the Gram-positive membrane model.

References

[1] N. A. Lerminiaux and A. D. S. Cameron, “Horizontal transfer of antibiotic resistance genes in clinical environments,” *Can. J. Microbiol.*, vol. 65, no. 1, pp. 34–44, 2019.

[2] W. Tsutomu, “Infective heredity of multiple drug resistance,” *Dep. Bacteriol. Keio Univ. Sch. Med. Tokyo, Japan*, vol. 27, no. 354, 1963.

[3] S. H. Podolsky, “The evolving response to antibiotic resistance (1945–2018),” *Palgrave Commun.*, vol. 4, no. 1, 2018.

[4] World Health Organization, *Global antimicrobial resistance surveillance system (GLASS) report: early implementation 2016-2017*. 2017.

[5] World Health Organization, “Global action plan on antimicrobial resistance,” *World Heal. Organ.*, pp. 1–28, 2017.

[6] “No time to wait: Securing the future from drug-resistant infections,” *Artforum International*. Interangency Coordination Group on Antimicrobial Resistance, 2019.

[7] D. M. P. De Oliveira *et al.*, “Antimicrobial Resistance in ESKAPE Pathogens.,” *Clin. Microbiol. Rev.*, vol. 33, no. 3, Jun. 2020.

[8] E. Tacconelli, “Global Priority List of Antibiotic-Resistant Bacteria to Guide Research, Discovery, and Development,” Infection Control Africa Network PP - South Africa, South Africa, 2017.

[9] R. J. Dubos, “Studies on a bactericidal agent extracted from a soil bacillus: II. Protective effect of the bactericidal agent against experimental pieuococcus infections in mice,” *J. Exp. Med.*, vol. 70, no. 1, pp. 11–18, 1939.

[10] R. D. Hotchkiss and R. J. Dubos, “Fractionation of the Bactericidal Agent From Cultures of a Soil Bacillus,” *J. Biol. Chem.*, vol. 132, no. 2, pp. 791–792, 1940.

[11] A. A. Bahar and D. Ren, “Antimicrobial peptides,” *Pharmaceuticals*, vol. 6, no. 12, pp. 1543–1575, 2013.

[12] J. Nissen-Meyer and I. F. Nes, “Ribosomally synthesized antimicrobial peptides: Their function, structure, biogenesis, and mechanism of action,” *Arch. Microbiol.*, vol. 167, no. 2–3, pp. 67–77, 1997.

[13] “PubMed - Search Results for antimicrobial peptides.” https://pubmed.ncbi.nlm.nih.gov/?term=antimicrobial+peptides&timeline=expanded (accessed Feb. 15, 2022).

[14] M. Mahlapuu, J. Håkansson, L. Ringstad, and C. Björn, “Antimicrobial peptides: An emerging category of therapeutic agents,” *Front. Cell. Infect. Microbiol.*, vol. 6, no. DEC, pp. 1–12, 2016.

[15] M. Hassan, M. Kjos, I. F. Nes, D. B. Diep, and F. Lotfipour, “Natural antimicrobial peptides from bacteria: Characteristics and potential applications to fight against antibiotic resistance,” *J. Appl. Microbiol.*, vol. 113, no. 4, pp. 723–736, 2012.

[16] M. Pasupuleti, A. Schmidtchen, and M. Malmsten, “Antimicrobial peptides: Key

components of the innate immune system," *Crit. Rev. Biotechnol.*, vol. 32, no. 2, pp. 143–171, 2012.

[17] V. Teixeira, M. J. Feio, and M. Bastos, "Role of lipids in the interaction of antimicrobial peptides with membranes," *Prog. Lipid Res.*, vol. 51, no. 2, pp. 149–177, 2012.

[18] T. Ebenhan, O. Gheysens, H. G. Kruger, J. R. Zeevaart, and M. M. Sathekge, "Antimicrobial Peptides: Their Role as Infection-Selective Tracers for Molecular Imaging," *Biomed Res. Int.*, vol. 2014, 2014.

[19] B. Bertani and N. Ruiz, "Function and Biogenesis of Lipopolysaccharides.," *EcoSal Plus*, vol. 8, no. 1, Aug. 2018.

[20] T. A. Soares and T. P. Straatsma, "Towards simulations of outer membrane proteins in lipopolysaccharide membranes," *AIP Conf. Proc.*, vol. 963, no. 2, pp. 1375–1378, 2007.

[21] R. E. W. Hancock, "Peptide antibiotics," *Lancet*, vol. 349, no. 9049, pp. 418–422, 1997.

[22] L. A. Clifton *et al.*, "Effect of divalent cation removal on the structure of gram-negative bacterial outer membrane models," *Langmuir*, vol. 31, no. 1, pp. 404–412, 2015.

[23] D. I. Andersson, D. Hughes, and J. Z. Kubicek-Sutherland, "Mechanisms and consequences of bacterial resistance to antimicrobial peptides," *Drug Resist. Updat.*, vol. 26, pp. 43–57, 2016.

[24] L. T. Nguyen, E. F. Haney, and H. J. Vogel, "The expanding scope of antimicrobial peptide structures and their modes of action," *Trends Biotechnol.*, vol. 29, no. 9, pp. 464–472, 2011.

[25] P. Kosikowska and A. Lesner, "Antimicrobial peptides (AMPs) as drug candidates: a patent review (2003–2015)," *Expert Opin. Ther. Pat.*, vol. 26, no. 6, pp. 689–702, 2016.

[26] Z. Jiang, A. I. Vasil, J. D. Hale, R. E. W. Hancock, M. L. Vasil, and R. S. Hodges, "Effects of net charge and the number of positively charged residues on the biological activity of amphipathic α-helical cationic antimicrobial peptides," *Biopolym. - Pept. Sci. Sect.*, vol. 90, no. 3, pp. 369–383, 2008.

[27] J. S. Gunn, S. S. Ryan, J. C. Van Velkinburgh, R. K. Ernst, and S. I. Miller, "Genetic and functional analysis of a PmrA-PmrB-regulated locus necessary for lipopolysaccharide modification, antimicrobial peptide resistance, and oral virulence of Salmonella enterica serovar typhimurium," *Infect. Immun.*, vol. 68, no. 11, pp. 6139–6146, 2000.

[28] M. Li, D. J. Cha, Y. Lai, A. E. Villaruz, D. E. Sturdevant, and M. Otto, "The antimicrobial peptide-sensing system aps of Staphylococcus aureus," *Mol. Microbiol.*, vol. 66, no. 5, pp. 1136–1147, 2007.

[29] S. M. Eswarappa, K. K. Panguluri, M. Hensel, and D. Chakravortty, "The yejABEF operon of Salmonella confers resistance to antimicrobial peptides and contributes to its virulence," *Microbiology*, vol. 154, no. 2, pp. 666–678, 2008.

[30] T. Guina, E. C. Yi, H. Wang, M. Hackett, and S. I. Miller, "A PhoP-regulated outer membrane protease of Salmonella enterica serovar typhimurium promotes resistance to alpha-helical antimicrobial peptides," *J. Bacteriol.*, vol. 182, no. 14, pp. 4077–4086, 2000.

[31] G. G. Perron, M. Zasloff, and G. Bell, "Experimental evolution of resistance to an antimicrobial peptide," *Proc. R. Soc. B Biol. Sci.*, vol. 273, no. 1583, pp. 251–256, 2006.

[32] R. Gläser, K. Becker, C. Von Eiff, U. Meyer-Hoffert, and J. Harder, "Decreased susceptibility of staphylococcus aureus small-colony variants toward human antimicrobial peptides," *J. Invest. Dermatol.*, vol. 134, no. 9, pp. 2347–2350, 2014.

[33] G. Shi *et al.*, "DRAMP 3.0: an enhanced comprehensive data repository of antimicrobial peptides.," *Nucleic Acids Res.*, vol. 50, no. D1, pp. D488–D496, Jan. 2022.

[34] V. Patrulea, G. Borchard, and O. Jordan, “An update on antimicrobial peptides (Amps) and their delivery strategies for wound infections,” *Pharmaceutics*, vol. 12, no. 9, pp. 1–39, 2020.

[35] A. Gomes, C. Teixeira, R. Ferraz, C. Prudencio, and P. Gomes, “Wound-healing peptides for treatment of chronic diabetic foot ulcers and other infected skin injuries,” *Molecules*, vol. 22, no. 10, pp. 1–18, 2017.

[36] H. B. Koo and J. Seo, “Antimicrobial peptides under clinical investigation,” *Pept. Sci.*, vol. 111, no. 5, 2019.

[37] A. K. Marr, W. J. Gooderham, and R. E. Hancock, “Antibacterial peptides for therapeutic use: obstacles and realistic outlook,” *Curr. Opin. Pharmacol.*, vol. 6, no. 5, pp. 468–472, 2006.

[38] G. S. Dijksteel, M. M. W. Ulrich, E. Middelkoop, and B. K. H. L. Boekema, “Review: Lessons Learned From Clinical Trials Using Antimicrobial Peptides (AMPs),” *Front. Microbiol.*, vol. 12, no. February, 2021.

[39] R. K. Thapa, D. B. Diep, and H. H. Tønnesen, “Topical antimicrobial peptide formulations for wound healing: Current developments and future prospects,” *Acta Biomater.*, vol. 103, pp. 52–67, 2020.

[40] C. L. Grek, G. M. Prasad, V. Viswanathan, D. G. Armstrong, R. G. Gourdie, and G. S. Ghatnekar, “Topical administration of a connexin43-based peptide augments healing of chronic neuropathic diabetic foot ulcers: A multicenter, randomized trial,” *Wound Repair Regen.*, vol. 23, no. 2, pp. 203–212, 2015.

[41] R. K. Thapa, D. B. Diep, and H. H. Tønnesen, “Nanomedicine-based antimicrobial peptide delivery for bacterial infections: recent advances and future prospects,” *J. Pharm. Investig.*, vol. 51, no. 4, pp. 377–398, 2021.

[42] S. Hamdan *et al.*, “Nanotechnology-Driven Therapeutic Interventions in Wound Healing: Potential Uses and Applications,” *ACS Cent. Sci.*, vol. 3, no. 3, pp. 163–175, 2017.

[43] L. Wang, C. Hu, and L. Shao, “The antimicrobial activity of nanoparticles: Present situation and prospects for the future,” *Int. J. Nanomedicine*, vol. 12, pp. 1227–1249, 2017.

[44] F. Danhier, E. Ansorena, J. M. Silva, R. Coco, A. Le Breton, and V. Préat, “PLGA-based nanoparticles: An overview of biomedical applications,” *J. Control. Release*, vol. 161, no. 2, pp. 505–522, 2012.

[45] J. S. Suk, Q. Xu, N. Kim, J. Hanes, and L. M. Ensign, “PEGylation as a strategy for improving nanoparticle-based drug and gene delivery,” *Adv. Drug Deliv. Rev.*, vol. 99, pp. 28–51, 2016.

[46] K. Zhang *et al.*, “PEG-PLGA copolymers: Their structure and structure-influenced drug delivery applications,” *J. Control. Release*, vol. 183, no. 1, pp. 77–86, 2014.

[47] C. Monteiro *et al.*, “A 17-mer Membrane-Active MSI-78 Derivative with Improved Selectivity toward Bacterial Cells,” *Mol. Pharm.*, vol. 12, no. 8, pp. 2904–2911, 2015.

[48] H. Li, T. Zhao, and Z. Sun, “Analytical techniques and methods for study of drug-lipid membrane interactions,” *Rev. Anal. Chem.*, vol. 37, no. 1, pp. 1–23, 2018.

[49] C. Peetla, A. Stine, and V. Labhasetwar, “Biophysical interactions with model lipid membranes: Applications in drug discovery and drug delivery,” *Mol. Pharm.*, vol. 6, no. 5, pp. 1264–1276, 2009.

[50] Y. H. M. Chan and S. G. Boxer, “Model membrane systems and their applications,” *Curr. Opin. Chem. Biol.*, vol. 11, no. 6, pp. 581–587, 2007.

[51] G. Brezesinski and H. Möhwald, “Langmuir monolayers to study interactions at model

membrane surfaces," *Adv. Colloid Interface Sci.*, vol. 100–102, no. SUPPL., pp. 563–584, 2003.

[52] E. Amado, A. Kerth, A. Blume, and J. Kressler, "Infrared reflection absorption spectroscopy coupled with brewster angle microscopy for studying interactions of amphiphilic triblock copolymers with phospholipid monolayers," *Langmuir*, vol. 24, no. 18, pp. 10041–10053, 2008.

[53] R. Maget-Dana, *The monolayer technique: A potent tool for studying the interfacial properties of antimicrobial and membrane-lytic peptides and their interactions with lipid membranes*, vol. 1462, no. 1–2. 1999.

[54] M. C. Giocondi and C. Le Grimellec, "Temperature Dependence of the Surface Topography in Dimyristoylphosphatidylcholine/Distearoylphosphatidylcholine Multibilayers," *Biophys. J.*, vol. 86, no. 4, pp. 2218–2230, 2004.

[55] A. Jesorka and O. Orwar, "Liposomes: Technologies and analytical applications," *Annu. Rev. Anal. Chem.*, vol. 1, no. 1, pp. 801–832, 2008.

[56] J. P. Reeves and R. M. Dowben, "Formation and properties of thin-walled phospholipid vesicles," *J. Cell. Physiol.*, vol. 73, no. 1, pp. 49–60, 1969.

[57] N. Rodriguez, F. Pincet, and S. Cribier, "Giant vesicles formed by gentle hydration and electroformation: A comparison by fluorescence microscopy," *Colloids Surfaces B Biointerfaces*, vol. 42, no. 2, pp. 125–130, 2005.

[58] K. Akashi, H. Miyata, H. Itoh, and K. Kinosita, "Preparation of giant liposomes in physiological saline and charcterization under an optical microscope," *Prog. Biophys. Mol. Biol.*, vol. 65, no. December, p. 220, 1996.

[59] K. Tsumoto, H. Matsuo, M. Tomita, and T. Yoshimura, "Efficient formation of giant liposomes through the gentle hydration of phosphatidylcholine films doped with sugar," *Colloids Surfaces B Biointerfaces*, vol. 68, no. 1, pp. 98–105, 2009.

[60] C. Billerit, G. D. M. Jeffries, O. Orwar, and A. Jesorka, "Formation of giant unilamellar vesicles from spin-coated lipid films by localized IR heating," *Soft Matter*, vol. 8, no. 42, pp. 10823–10826, 2012.

[61] J. I. Pavlič, J. Genova, G. Popkirov, V. Kralj-Iglič, A. Iglič, and M. D. Mitov, "Mechanoformation of neutral giant phospholipid vesicles in high ionic strength solution," *Chem. Phys. Lipids*, vol. 164, no. 8, pp. 727–731, 2011.

[62] J. R. Howse, R. A. L. Jones, G. Battaglia, R. E. Ducker, G. J. Leggett, and A. J. Ryan, "Templated formation of giant polymer vesicles with controlled size distributions," *Nat. Mater.*, vol. 8, no. 6, pp. 507–511, 2009.

[63] K. S. Horger, D. J. Estes, R. Capone, and M. Mayer, "Films of agarose enable rapid formation of giant liposomes in solutions of physiologic ionic strength," *J. Am. Chem. Soc.*, vol. 131, no. 5, pp. 1810–1819, 2009.

[64] T. P. T. Dao *et al.*, "Membrane properties of giant polymer and lipid vesicles obtained by electroformation and pva gel-assisted hydration methods," *Colloids Surfaces A Physicochem. Eng. Asp.*, vol. 533, no. July, pp. 347–353, 2017.

[65] N. L. Mora *et al.*, "Preparation of size tunable giant vesicles from cross-linked dextran(ethylene glycol) hydrogels," *Chem. Commun.*, vol. 50, no. 16, pp. 1953–1955, 2014.

[66] M. I. Angelova and D. S. Dimitrov, "Liposome Electro formation," pp. 303–311, 1986.

[67] R. Dimova, P. Stano, C. M. Marques, and P. Walde, "Preparation methods for giant unilamellar vesicles," *Giant Vesicle B.*, pp. 3–20, 2020.

[68] S. Aden, T. Snoj, and G. Anderluh, "The use of giant unilamellar vesicles to study

functional properties of pore-forming toxins," *Methods Enzymol.*, vol. 649, pp. 219–251, 2021.

[69] S. Pautot, B. J. Frisken, and D. A. Weitz, "Engineering asymmetric vesicles," *Proc. Natl. Acad. Sci. U. S. A.*, vol. 100, no. 19, pp. 10718–10721, 2003.

[70] P. Walde, K. Cosentino, H. Engel, and P. Stano, "Giant Vesicles: Preparations and Applications," *ChemBioChem*, vol. 11, no. 7, pp. 848–865, 2010.

[71] H. Saito *et al.*, "Time-resolved tracking of a minimum gene expression system reconstituted in giant liposomes," *ChemBioChem*, vol. 10, no. 10, pp. 1640–1643, 2009.

[72] D. Merkle, N. Kahya, and P. Schwille, "Reconstitution and anchoring of cytoskeleton inside giant unilamellar vesicles.," *Chembiochem*, vol. 9, no. 16, pp. 2673–2681, 2008.

[73] H. H. Zepik, P. Walde, E. L. Kostoryz, J. Code, and D. M. Yourtee, "Lipid vesicles as membrane models for toxicological assessment of xenobiotics," *Crit. Rev. Toxicol.*, vol. 38, no. 1, pp. 1–11, 2008.

[74] M. Sakamoto, A. Shoji, and M. Sugawara, "Giant unilamellar vesicles containing Rhodamine 6G as a marker for immunoassay of bovine serum albumin and lipocalin-2," *Anal. Biochem.*, vol. 505, pp. 66–72, 2016.

[75] Y. Tamba and M. Yamazaki, "Single giant unilamellar vesicle method reveals effect of antimicrobial peptide magainin 2 on membrane permeability," *Biochemistry*, vol. 44, no. 48, pp. 15823–15833, 2005.

[76] A. Verchère, I. Broutin, and M. Picard, "Reconstitution of membrane proteins in liposomes," *Methods Mol. Biol.*, vol. 1635, no. 2000, pp. 259–282, 2017.

[77] M. Pinheiro *et al.*, "Differential interactions of rifabutin with human and bacterial membranes: Implication for its therapeutic and toxic effects," *J. Med. Chem.*, vol. 56, no. 2, pp. 417–426, 2013.

[78] I. D. Alves *et al.*, "Membrane interaction and perturbation mechanisms induced by two cationic cell penetrating peptides with distinct charge distribution," *Biochim. Biophys. Acta - Gen. Subj.*, vol. 1780, no. 7–8, pp. 948–959, 2008.

[79] C. Montis *et al.*, "Multifunctional nanoassemblies target bacterial lipopolysaccharides for enhanced antimicrobial DNA delivery," *Colloids Surfaces B Biointerfaces*, vol. 195, no. July, pp. 1–10, 2020.

[80] P. Costa, "Nanoplatforms role in bacterial infections : design and development of new delivery systems and membrane mimetic models", M. S. thesis, Faculdade de Engenharia da Universidade do Porto, 2020.

[81] X. Wu, P. H. Wei, X. Zhu, M. J. Wirth, A. Bhunia, and G. Narsimhan, "Effect of immobilization on the antimicrobial activity of a cysteine-terminated antimicrobial Peptide Cecropin P1 tethered to silica nanoparticle against E. coli O157:H7 EDL933," *Colloids Surfaces B Biointerfaces*, vol. 156, pp. 305–312, 2017.

[82] W. Guo *et al.*, "Probing Molecular Interactions between Surface-Immobilized Antimicrobial Peptides and Lipopolysaccharides in Situ," *Langmuir*, vol. 36, no. 41, pp. 12383–12393, 2020.

[83] H. Stein, S. Spindler, N. Bonakdar, C. Wang, and V. Sandoghdar, "Production of Isolated Giant Unilamellar Vesicles under High Salt Concentrations.," *Front. Physiol.*, vol. 8, p. 63, 2017.

[84] K. Tahara, S. Tadokoro, Y. Kawashima, and N. Hirashima, "Endocytosis-like uptake of surface-modified drug nanocarriers into giant unilamellar vesicles," *Langmuir*, vol. 28, no. 18, pp. 7114–7118, 2012.

[85] S. J. Parikh and J. Chorover, "Infrared spectroscopy studies of cation effects on

lipopolysaccharides in aqueous solution," *Colloids Surfaces B Biointerfaces*, vol. 55, no. 2, pp. 241–250, 2007.

[86] A. Barkleit, H. Foerstendorf, B. Li, A. Rossberg, H. Moll, and G. Bernhard, "Coordination of uranium(vi) with functional groups of bacterial lipopolysaccharide studied by EXAFS and FT-IR spectroscopy," *Dalt. Trans.*, vol. 40, no. 38, pp. 9868–9876, 2011.

[87] A. Ramôa, "Antimicrobial Nanoparticles to Fight Bacterial Wound Infections", M. S. thesis, Faculdade de Engenharia da universidade do Porto, 2021.